into consideration during drug development to improve brain penetration and to avoid drug-drug interactions involving these transporters and subsequent side effects. In general, BBB permeability increases with increasing lipophilicity because the passive entry of molecules into the brain increases. However, a number of highly lipophilic drugs demonstrate unexpectedly poor BBB penetration because they are effluxed by P-gp. An approach to increase lipophilicity is not always useful as far as improving brain penetration is concerned. Brain penetration of drugs that pharmacologically target the CNS could, therefore, be improved by modifying the drug so that it is not recognized by P-gp (Doan et al., 2002). Whether poor brain penetration of a drug is due to poor membrane permeability or active efflux should be investigated in detail at an early stage of drug development. The expression system of transporters is an efficient tool for screening transport activities. Human transporter gene transfected cells are especially important tools because human experimental systems are rather limited. Recent studies show that the transport activity of MDR1-transfected cells correlates well with the P-gp transport activity in vivo (Adachi et al., 2001; Yamazaki et al., 2001).

However, reducing brain penetration by efflux transporters is expected to enable the adverse CNS side effects to be avoided in some drugs with toxic CNS effects. Some fluoroquinolone antibacterials or anticancer agents exhibit low brain distribution, despite having a high lipophilicity, because they are prevented from entering the brain by P-gp (Tamai and Tsuji, 2000). This probably explains their relative lack of CNS side effects. The brain uptake of ivermectin is markedly increased (27-fold) in mdr1a knockout mice (Table 4). Mdr1a knockout mice are much more sensitive (100-fold) than normal mice to the neurotoxic effects caused by ivermectin (Schinkel et al., 1994). Drug design, which ensures that the compounds interact with brain efflux transporter, may be a successful way to avoid the CNS toxicity of drug candidates that exhibit such an effect. However, a drug-drug interaction involving P-gp or a genetic polymorphism of MDR1 may change the brain penetration of drugs and may affect safety if the drug candidate is a P-gp substrate. Thus, it is important to select a lead compound that has no intrinsic CNS toxic potential rather than targeting the brain efflux transporter. Drug-drug interactions via brain P-gp between loperamide, a substrate for P-gp, and quinidine, an inhibitor of P-gp, have been reported (Sadeque et al., 2000). Although the antidiarrheal agent loperamide is a potent opiate, it does not produce opioid CNS effects at usual doses in patients. When a 16-mg dose of loperamide alone was administered to eight healthy volunteers, loperamide produced no respiratory depression. However, respiratory depression occurred when loperamide (16 mg) was given with quinidine at a dose of 600 mg. These changes were not explained by increased plasma loperamide concentrations. Thus, inhibition of P-gp by quinidine increases the entry of loperamide into the CNS with resulting opiate-induced respiratory depression. The lack of respiratory depression produced by loperamide, which allows it to be safely used therapeutically, can be reversed by a drug-drug interaction mediated by P-gp, resulting in serious toxic and abuse potential.

In addition, some organic anion-transporting polypeptides (OATPs) are expressed in the brain. Many members of this transporter family mediate transport of a wide spectrum of amphipathic organic anions (Hagenbuch and Meier, 2003). Rat Oatp2 (*Slc21a5*) is localized on both the luminal and abluminal membranes of the rat BBB (Gao et al., 1999). In humans, immunohistochemical staining of brain tissue suggested that OATP-A is expressed in the brain endothelial cells, although its localization has not been confirmed (Gao et al., 2000). Because Oatp2 can mediate bidirectional transport, involvement of Oatp2 in the efflux transport across the BBB is possible (Asaba et al., 2000; Sugiyama et al., 2001). The recently characterized human OATP-F is a high-affinity thyroxine transporter and is selectively expressed in brain (Pizzagalli et al., 2002). OATP-F is possibly involved in the uptake of thyroxin from the blood into the CNS. Moreover, OAT3, OCT3, and OCTN2 appear to be expressed in the brain (Wu et al., 1998; Kusuhara et al., 1999; Wu et al., 1999; Cha et al., 2001; Ohtsuki et al., 2002). Their localization in the brain and physiological function remain to be elucidated. It is essential to identify most of the important transporters in the brain and to characterize their function to provide a basis for developing strategies to regulate drug disposition in the brain.

C. Role of Transporters in Drug Absorption

Various transporters are expressed in the brush-border membranes of intestinal epithelial cells (Table 1). They are involved in the efficient absorption of nutrients or endogenous compounds. The use of influx transporters expressed in the gut, such as PEPT1, ASBT, OATP-B, OATP-D, OATP-E, or rat Oatp3 (*Slc21a7*), will help improve drug absorption (Tsuji and Tamai, 1996; Oh et al., 1999; Tamai et al., 2000a; Walters et al., 2000; Kullak-Ublick et al., 2001; Lee et al., 2001b). Rat Oatp3, but not Oatp1 (*Slc21a1*) or Oatp2, is expressed in the small intestine, and is localized on the apical brush-border membrane of enterocytes (Walters et al., 2000). Because Oatp3 transports taurocholate, rat oatp3 is suggested to mediate the absorption of bile acids. PEPT1 mediates the transport of peptide-like drugs such as β-lactam antibiotics, angiotensin-converting enzyme (ACE) inhibitors and the dipeptide-like anticancer drug bestatin (Hori et al., 1993; Saito and Inui, 1995; Swaan et al., 1995; Terada et al., 1997; Inui et al., 2000b). Interestingly, valacyclovir, a valyl ester prodrug of the antiviral agent acyclovir, although it does not contain a peptide bond, is transported by PEPT1 (Balimane et al.,

TABLE 4
$K_{p,brain}$ *values in mdr1a(−/−) and mdr1a(+/+) mice after intravenous injection of various drugs*

	Time after administration	mdr1a(+/+)			mdr1a(−/−)			Ratio ($K_{p,brain,ko}$/ $K_{p,brain,wt}$)	Reference
		Plasma Conc. (ng/ml)	Brain Conc. (ng/ml)	$K_{p,brain}$	Plasma Conc. (ng/ml)	Brain Conc. (ng/ml)	$K_{p,brain}$		
Asimadoline[a]	1 h	211	65	0.31	199	586	2.94	9.56	Jonker et al., 1999
Azasetron				0.119			0.833	7.0	Tamai and Tsuji, 2000
Carebastin				0.0403			0.319	7.9	Tamai and Tsuji, 2000
Cyclosporine	4 h	38	10.5	0.28	54	178	3.3	12	Schinkel et al., 1995b
Daunomycin	30 min			0.91			1.63	1.8	Adachi et al., 2001
Dexamethasone	4 h	17.2	4.9	0.28	17.2	12.1	0.7	2.5	Schinkel et al., 1995b
Diazepam	30 min			3.35			3.24	0.9	Adachi et al., 2001
Digoxin	4 h	669	55.5	0.08	1259	1939	1.5	19	Schinkel et al., 1995b
Digoxin	90 min	21.2	1.1	0.05	39.6	21.1	0.53	10.3	Mayer et al., 1997
Digoxin[a]	4 h	622	37.1	0.06	1775	1011	0.57	9.5	Schinkel et al., 1997
Doxorubicin	1 h			0.00077			0.0025	3.2	Kusuhara and Sugiyama, 2001a
Ebastine				0.114			0.846	7.4	Tamai and Tsuji, 2000
Grepafloxacin[a,b]	2 h			0.34			1	2.9	Tamai et al., 2000b
HSR903	2 h			0.38			2.85	7.5	Murata et al., 1999
Indinavir	4 h	19	1.6	0.08	21	17	0.81	10	Kim et al., 1998
Ivermectin[c]	4 h	22	0.9	0.041	70	41	0.586	14.3	Schinkel et al., 1995a
Ivermectin[c]	24 h	16	1.5	0.094	52	131	2.519	26.9	Schinkel et al., 1994
Loperamide[c]	4 h	13.3	4.1	0.31	26.7	55.3	2.1	6.7	Schinkel et al., 1996
Morphine	4 h	10.9	5.3	0.49	12.4	8.9	0.72	1.48	Schinkel et al., 1995b
Nelfinavir	4 h	14	1.2	0.09	17	45	2.65	31	Kim et al., 1998
Ondansetron	30 min	40.5	18.7	0.46	39.4	75.6	1.92	4.2	Schinkel et al., 1996
Progesterone	30 min			1.45			1.34	0.9	Adachi et al., 2001
Quinidine	10 min			0.17			4.64	28	Kusuhara et al., 1997
Rhodamine-123	4 h	2.55	0.54	0.21	2.84	2.81	0.99	4.66	de Lange et al., 1998
Saquinavir	4 h	31	4.1	0.13	34	30	0.88	6.67	Kim et al., 1998
Sparfloxacin[a,b]	2 h			0.14			0.54	3.9	Tamai et al., 2000b
Tacrolimus	5 h			2.73			16.4	6.1	Yokogawa et al., 1999
Valspodar	4 h			0.6			1.2	2	Desrayaud et al., 1998
Verapamil	1 h	35	15	0.42	43	142	3.3	7.9	Hendrikse et al., 1998
Vinblastine	4 h	3	5	1.7	6	112	18.7	11	Schinkel et al., 1994
Vincristine				0.027			0.066	2.4	Tamai and Tsuji, 2000

Drugs were administered intravenously to both wild-type and mdr1a or mdr1a/1b double knockout mice. Plasma and brain concentrations were determined at the time of death. $K_{p,brain}$ was obtained by dividing the brain concentration by the plasma concentration.
[a] Mdr1a/mdr1b double knockout mice were used for this experiment.
[b] $K_{p,brain}$ values of grepafloxacin and sparfloxacin were evaluated using plasma unbound concentration.
[c] Oral administration.

1998; Sawada et al., 1999). From the viewpoint of drug delivery, L-valyl esterification of poorly absorbed drugs has been suggested as a useful strategy for improving their bioavailability and therapeutic efficacy.

However, primary active efflux transporters, such as P-gp, MRP2, or BCRP, are expressed on the brush-border membrane of enterocytes (Table 1) and excrete their substrates into the lumen, resulting in a potential limitation of net absorption (Gotoh et al., 2000; Hirohashi et al., 2000a; Jonker et al., 2000; Taipalensuu et al., 2001). Active secretion of absorbed drug is now becoming recognized as a significant factor in oral drug bioavailability (Wacher et al., 2001; Zhang and Benet, 2001). P-gp contributes to the absorption of many drugs because of its broad substrate specificity (Borst et al., 1999; Fromm, 2000; Troutman et al., 2001). The intestinal P-gp content correlates with the AUC after oral administration of digoxin, a P-gp substrate, in humans (Greiner et al., 1999). This result suggests that P-gp in the epithelium of the gut wall determines the plasma concentration of orally administered digoxin. Another report involving a patient undergoing a small bowel transplant has also demonstrated that the plasma concentration of orally administered tacrolimus, a substrate of both P-gp and CYP3A4, correlated well with the mRNA expression of intestinal MDR1, but not CYP3A4 (Masuda et al., 2000). These results suggest that intestinal P-gp, rather than CYP3A4, is a good probe to predict intraindividual variations in tacrolimus pharmacokinetics. Furthermore, high levels of MDR1 are strongly associated with reductions in survival rates after living-donor liver transplantation and subsequent immunosuppressive therapy with tacrolimus (Hashida et al., 2001). Intestinal MDR1 is also a powerful prognostic indicator of living-donor liver transplantation outcomes.

BCRP is a multidrug-resistance protein that is a new member of the ATP-binding cassette transporter family (Doyle et al., 1998). BCRP has only one ATP-binding cassette and six putative transmembrane domains (Rocchi et al., 2000), suggesting that BCRP is a half-transporter, which may function as a homo- or heterodimer. BCRP plays a role in the secretion of clinically important drugs such as topotecan (Jonker et al., 2000). When both topotecan, a substrate of BCRP, and GF120918, an inhibitor of both BCRP and P-gp, were administered orally, the bioavailability of topotecan was increased in P-gp-deficient mice (over 6-fold) compared with mice

given vehicle alone (Jonker et al., 2000) (Table 5). Thus, BCRP appears to be a major determinant of the bioavailability of topotecan following oral administration. Because GF120918 inhibits both P-gp and BCRP, P-gp-deficient mice have been used to exclude any confounding effects of P-gp inhibition. Topotecan is a weak-to-moderate substrate of P-gp, thus P-gp also appears to play a role in the bioavailability of topotecan. BCRP is expressed not only in the intestine, but also in the bile canalicular membrane and placenta (Maliepaard et al., 2001). Thus, treatment with GF120918 reduced the plasma clearance and hepatobiliary excretion of topotecan (Table 5). Furthermore, in pregnant GF120918-treated, P-gp-deficient mice, the fetal penetration of topotecan was 2-fold higher than that in pregnant mice given vehicle alone (Maliepaard et al., 2001). These results indicate that BCRP plays an important role in protecting the fetus from topotecan. The bioavailability of topotecan in humans is moderate, with a high interpatient variability (30 ± 8%) (Schellens et al., 1996). By combining oral topotecan with an effective BCRP inhibitor, the bioavailability of topotecan might be markedly improved and the interindividual variability might be reduced (de Bruin et al., 1999). Although GF120918 inhibits not only BCRP but also P-gp, fumitremorgin C, an extract of *Aspergillus fumigatus,* has been shown to potently inhibit BCRP but not P-gp or MRP, suggesting that fumitremorgin C is a highly selective inhibitor of BCRP (Rabindran et al., 1998; Ozvegy et al., 2001). So, the strategic application of BCRP inhibitors may lead to more effective oral chemotherapy with topotecan or other drugs that are BCRP substrates.

In principle, the inhibition of intestinal efflux transporters is a useful way to improve the oral bioavailability of a coadministered drug (Sikic et al., 2000). It has been shown that treatment with water-soluble vitamin E (*d*-α-tocopheryl polyethylene glycol 1000 succinate [TPGS]) enhances the absorption of cyclosporine in healthy volunteers or liver transplant recipients (Sokol et al., 1991; Chang et al., 1996). Another report has demonstrated that TPGS also increased the solubility of amprenavir, an HIV protease inhibitor, and inhibited the efflux transport systems and enhanced the permeability of amprenavir through Caco-2 cell monolayers (Yu et al., 1999). Overall, TPGS enhances the absorption flux of amprenavir by increasing its solubility and permeability. This improvement is very significant since the bioavailability of amprenavir in conventional capsule formulations is almost zero, and the softgel formulation containing vitamin E-TPGS is 69% bioavailable for dogs (Yu et al., 1999). Surfactants, such as Cremophor EL or Tween 80, have been found to be potent inhibitors of P-gp (Lo et al., 1998; van Zuylen et al., 2001). Both are used as formulation vehicles for a variety of poorly water-soluble drugs, including the anticancer agents paclitaxel and docetaxel. The use of these surfactants may increase the intestinal absorption of some drugs through P-gp inhibition and, thus, improve the drug bioavailability of P-gp substrates.

TABLE 5
Effect of BCRP inhibitor GF120918 on pharmacokinetics of topotecan in mdr1a/1b(−/−) mice (Jonker et al., 2000)

	Vehicle-Treated	GF120918-Treated	Ratio
Oral administration of topotecan (1 mg/kg)[a]			
AUC (mg · h/l)	96	596	×6.2
Intravenous administration of topotecan (1 mg/kg)[a]			
AUC (mg · h/l)	200	406	×2.0
Biliary excretion[b] (%)	14.7	5.5	×0.4
Intestinal content of [^{14}C]topotecan-derived radioactivity[c]			
Intestinal (%)	31.8	10.2	×0.3
Plasma (ng/ml)	40	102	×2.6

[a] Mdr1a/1b(−/−) mice were given an oral dose of GF120918 (50 mg/kg) or vehicle 15 min before an oral or intravenous dose of topotecan (1 mg/kg).
[b] Cumulative biliary excretion of unchanged topotecan for 11 min.
[c] GF120918 (50 mg/kg) was administered orally; 15 min later, [^{14}C]topotecan (1 mg/kg) was administered intravenously; 60 min after administration of [^{14}C]topotecan, the intestinal content of [^{14}C] was determined.

Inhibition studies using P-gp inhibitors in Caco-2 cell monolayers are simple to perform and are widely used to evaluate the contribution of P-gp to the absorption of a drug candidate. However, there are few studies describing any quantitative investigations or the theoretical aspects involved. Table 6 shows the effect of P-gp inhibitors on the apical-to-basal or basal-to-apical flux of P-gp substrates across Caco-2 cell monolayers. As a result, the changes in the flux of P-gp substrates can be classified into three types (Fig. 1). In the first type, the basal-to-apical flux scarcely changes and the apical-to-basal flux increases markedly in the presence of a P-gp inhibitor (Fig. 1A). In the second case, both fluxes are changed but the degree of change in the apical-to-basal flux is greater than that in the basal-to-apical flux in the presence of a P-gp inhibitor (Fig. 1B). In the third case, both fluxes are changed but the degree of change in the basal-to-apical flux is greater than that in the apical-to-basal flux in the presence of a P-gp inhibitor (Fig. 1C). An example of the first case is grepafloxacin, the second case is illustrated by saquinavir and indinavir, while examples of the third case include Rhodamine 123, cyclosporine, vinblastine, and digoxin (Table 6). Figure 2 shows a schematic diagram illustrating the transcellular transport of P-gp substrates in Caco-2 cell monolayers. PS_1 and PS_2 represent the permeability-surface area (PS) products for the influx and non-P-gp-mediated efflux across the apical membrane of Caco-2 cell monolayers, respectively; PS_3 and PS_4 represent the PS products for the efflux and influx across the basal membrane of Caco-2 cell monolayers, respectively; and $PS_{P\text{-}gp}$ represents the PS product for P-gp-mediated efflux across the apical membrane. $CL_{A\text{-}B}$ and $CL_{B\text{-}A}$ represent the steady-state transport clearances in the apical-to-basal direction and the basal-to-apical direction, respectively. Supposing a steady-state flux (constant velocity of tran-

TABLE 6
The effects of P-gp inhibitors on transcellular transport of P-gp substrates in Caco-2 cell monolayers

Substrate (μM)	Inhibitor (μM)	−Inhibitor[a]		R_{caco}(−I)	+Inhibitor[a]		R_{caco} (+I)	Ratio(+I/cont)		Type[b]	Reference
		A-B	B-A	B-A/A-B	A-B	B-A	B-A/A-B	A-B	B-A		
Grepafloxacin (5)	Grepafloxacin 1000	0.6	2.1	3.4	1.7	1.6	0.9	2.77	0.76	A	Yamaguchi et al., 2000
Saquinavir (5)	PSC-833 1	2.3	22.8	9.8	8.8	12.9	1.5	3.78	0.57	B	Kim et al., 1998
Indinavir (5)	PSC-833 1	1.7	18.4	11	7.0	10.6	1.5	4.20	0.58	B	Kim et al., 1998
Rhodamine-123 (5)	Verapamil 100	0.1	3.7	34	0.3	0.3	1.3	2.46	0.09	C	Takano et al., 1998
Cyclosporine (1)	Verapamil 100	3.5	25.4	7.2	6.4	7.5	1.2	1.80	0.30	C	Alsenz et al., 1998
Vinblastine (0)	GF120918 10	3.8	12.9	3.4	6.2	5.9	1.0	1.61	0.46	C	Lentz et al., 2000
Digoxin (5)	CP114416 1	1.6	12.5	7.7	4.2	3.5	0.8	2.57	0.28	C	Wandel et al., 1999

[a] Papp ($\times 10^{-6}$ cm/s).
[b] Classification types for the effect of P-gp inhibitors on the transcellular transport of P-gp substrates shown in Fig. 1.

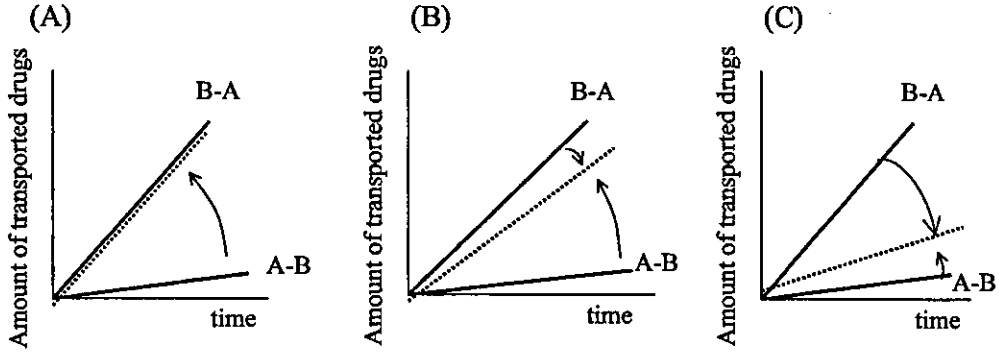

FIG. 1. Schematic diagram illustrating the effect of P-gp inhibitors on the apical-to-basal (A-B) or basal-to-apical (B-A) flux of P-gp substrates across Caco-2 cell monolayers. The changes in the flux of P-gp substrates can be classified into three types (A–C). Solid lines or dotted lines represent the flux across monolayers without or with P-gp inhibitors, respectively. Three classification types can be interpreted according to eqs. 1–5 shown in Fig. 2

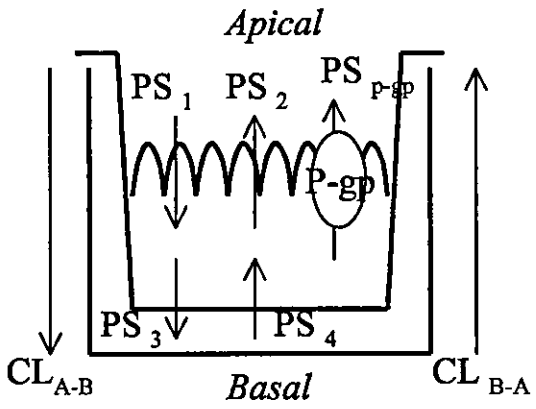

$$CL_{A\text{-}B} = \frac{PS_1 \times PS_3}{(PS_2 + PS_{P\text{-}gp}) + PS_3} \quad \text{(Eq. 1)}$$

$$CL_{B\text{-}A} = \frac{PS_4 \times (PS_2 + PS_{P\text{-}gp})}{(PS_2 + PS_{P\text{-}gp}) + PS_3} \quad \text{(Eq. 2)}$$

$$R_{caco} = \frac{CL_{B\text{-}A}}{CL_{A\text{-}B}} = \frac{PS_4 \times (PS_2 + PS_{P\text{-}gp})}{PS_1 \times PS_3} \quad \text{(Eq. 3)}$$

$$\frac{CL_{A\text{-}B}(+I)}{CL_{A\text{-}B}(cont)} = \frac{(PS_2 + PS_{P\text{-}gp}) + PS_3}{PS_2 + PS_3} \quad \text{(Eq. 4)}$$

$$\frac{CL_{B\text{-}A}(+I)}{CL_{B\text{-}A}(cont)} = \frac{PS_2 \times ((PS_2 + PS_{P\text{-}gp}) + PS_3)}{(PS_2 + PS_3)(PS_2 + PS_{P\text{-}gp})} \quad \text{(Eq. 5)}$$

FIG. 2. Schematic diagram illustrating transcellular transport of P-gp substrates in Caco-2 cell monolayers. PS_1 and PS_2 represent the permeability-surface area (PS) products for the influx and non-P-gp-mediated efflux across the apical membrane of the cell monolayers, respectively. PS_3 and PS_4 represent the PS products for the efflux and influx across the basal membrane of the cell monolayers, respectively. $PS_{P\text{-}gp}$ represents the PS product for P-gp-mediated efflux across the apical membrane. $CL_{A\text{-}B}$ and $CL_{B\text{-}A}$ represent the steady-state clearances across the monolayers in the apical-to-basal direction and the basal-to-apical direction, respectively. $CL_{A\text{-}B}(+I)$ and $CL_{B\text{-}A}(+I)$ represent the steady-state transport clearances when P-gp is completely inhibited by a P-gp inhibitor.

scellular transport) and "sink" conditions (constant concentration gradients), $CL_{A\text{-}B}$ and $CL_{B\text{-}A}$ are given by eqs. 1 and 2 of Fig. 2, respectively. The flux ratio across the monolayer (R_{caco}), defined as the ratio of $CL_{A\text{-}B}$ to $CL_{B\text{-}A}$, is given by eq. 3 of Fig. 2. The degree of change in $CL_{A\text{-}B}$ and $CL_{B\text{-}A}$, when P-gp in completely inhibited by P-gp inhibitor, is given by eqs. 4 and 5 of Fig. 2, respectively. $CL_{A\text{-}B}(+I)$ and $CL_{B\text{-}A}(+I)$ represent the clearances when

P-gp is completely inhibited by a P-gp inhibitor. The experimental data in Table 6 can be interpreted using eqs. 3 to 5 of Fig. 2, where it has been estimated that $PS_2 \gg PS_3$ in the first case (Fig. 1A), $PS_2 \fallingdotseq PS_3$ in the second case (Fig. 1B), and $PS_2 \ll PS_3$ in the third case (Fig. 1C). Furthermore, it has been estimated that the value of $PS_{P\text{-}gp}$ is 2-fold greater in the case of grepafloxacin, 6- to 8-fold greater in the case of saquinavir and indinavir, and 6- to 21-fold greater in case of Rhodamine 123, cyclosporine, vinblastine, and digoxin compared with the non-P-gp-mediated efflux clearance (PS_2). In some cases, it has been found that the basal-to-apical flux is still greater than the apical-to-basal flux with P-gp inhibitors. The reason for this phenomenon may be not only that the inhibitor concentration is insufficient, but also that the efflux transporters on the apical membrane, other than P-gp, also play a role in the efflux of these drugs.

D. Control of Elimination by Drug Transporters (Uptake and Efflux Transporters in the Liver and Kidney)

Multispecific transporters are expressed in the liver and kidney and play an important role in the elimination of many xenobiotics, acting as a detoxification system. Many drugs are excreted into the urine via organic anion and cation transport systems, expressed on brush-border and basolateral membranes of renal tubular cells (Table 1) (Burckhardt and Wolff, 2000; Inui et al., 2000a; Sekine et al., 2000; van Aubel et al., 2000; Dresser et al., 2001; Masereeuw and Russel, 2001; Russel et al., 2002). As far as the liver is concerned, a wide variety of transporter families are known to be present at the sinusoidal and canalicular membranes and play a significant role in hepatobiliary excretion (Table 1) (Oude Elferink et al., 1995; Yamazaki et al., 1996; Muller and Jansen, 1997; Keppler and Konig, 2000; Kullak-Ublick et al., 2000; Faber et al., 2003). Secondary active transporters expressed on the sinusoidal membrane are responsible for the uptake of drugs from the blood into hepatocytes (Meier et al., 1997). Primary active transporters expressed on the canalicular membrane are involved in the biliary excretion of both parent drugs and their metabolites (Kusuhara et al., 1998; Hooiveld et al., 2001). Since some transporters are specifically expressed on hepatocytes or renal tubular cells, they can be used as a target for drug delivery to the liver or kidney, possibly resulting in direct control of the elimination process. The transporters expressed in the liver and kidney are introduced here.

1. Organic Anion Transporting Polypeptide (SLC21A) Family. Organic anion transporting polypeptides (OATPs) have been isolated from rats, at first as candidates for the sodium-independent uptake system in the liver (Meier et al., 1997; Muller and Jansen, 1997). OATPs form a growing gene superfamily and mediate transport of a wide spectrum of amphipathic organic anions such as bromosulfophthalein, estradiol-17β-glucuronide (E_2-17βG), bile acids, thyroid hormones, and drugs such as pravastatin, temocaprilat, and BQ-123 (Meier et al., 1997; Muller and Jansen, 1997; Ishizuka et al., 1998; Kakyo et al., 1999; Reichel et al., 1999; Abu-Zahra et al., 2000). Although some important members of this transporter superfamily are selectively expressed in rodent and human livers, most OATPs are expressed in multiple tissues including the BBB, choroid plexus, lung, heart, intestine, kidney, placenta, and testes (Hagenbuch and Meier, 2003). A human OATP-C (also referred to as OATP2 and LST-1) is predominantly expressed in the liver (Abe et al., 1999; Hsiang et al., 1999; Konig et al., 2000a; Tamai et al., 2000a). Due to its broad substrate specificity, OATP-C is considered to play a major role in the hepatic uptake of organic anions. Recently, Cui et al. demonstrated that OATP-C transports bilirubin and its mono- and diglucuronide, suggesting that OATP-C is important from a physiological point of view (Cui et al., 2001b). In addition to OATP-C, OATP-B and OATP8 are also localized on the sinusoidal membrane of hepatocytes (Table 1) (Konig et al., 2000b; Kullak-Ublick et al., 2001). The tissue distribution of OATP-B is much broader than that of liver specific OATP-C. Although the expression of OATP-B is most abundant in human liver, it is also present in the pancreas, lung, gut, ovary, testes, and spleen. (Tamai et al., 2000a; Kullak-Ublick et al., 2001; St-Pierre et al., 2002). OATP-B transports sulfate conjugates of steroids, but not glucuronide conjugates and bile salts, whereas OATP-C transports both types of steroid conjugates (Kullak-Ublick et al., 2001; Tamai et al., 2001). OATP8 is exclusively expressed on the basolateral membrane of hepatocytes (Konig et al., 2000b). Although OATP-C and OATP8 exhibit broad overlapping substrate specificities, OATP8 is unique in transporting digoxin and exhibits an especially high transport activity for anionic peptides [D-penicillamine(2,5)] enkephalin (opioid-receptor agonist), BQ-123 (endothelin-receptor antagonist), and cholecystokinin-8 (gastrointestinal peptide hormone 8) (Ismair et al., 2001; Kullak-Ublick et al., 2001). The bile salts, substrates for OATP-C, are reportedly not transported by OATP8 (Konig et al., 2000b). Because OATP-C, OATP-B, and OATP8 are localized on the same membrane domain with overlapping substrate specificity, the contribution of OATP-C, OATP-B, and OATP8 to the total hepatic uptake of each ligand needs to be clarified.

2. Organic Anion Transporter (SLC22A) Family. OAT1 and OAT3 are mainly expressed in the kidney and localized on the basolateral membrane of the proximal tubules (Table 1) (Sekine et al., 1997; Hosoyamada et al., 1999; Kusuhara et al., 1999; Sekine et al., 2000; van Aubel et al., 2000; Dresser et al., 2001; Kojima et al., 2002). Their substrates include relatively small and hydrophilic organic anions, such as *p*-aminohippurate (PAH), methotrexate, β-lactam antibiotics, nonste-

roidal anti-inflammatory drugs (NSAIDs), and antiviral nucleoside analogs (Uwai et al., 1998; Apiwattanakul et al., 1999; Cihlar et al., 1999; Jariyawat et al., 1999; Wada et al., 2000). Recently, Oat3 knockout mice have been developed, and Oat3$^{-/-}$ mice exhibit impaired organic anion transport function in renal and choroid plexus epithelia but not in the liver (Sweet et al., 2002). This indicates that Oat3 plays an essential role in renal, but not hepatic, organic anion uptake.

Generally, amphipathic organic anions with a relatively high molecular weight, such as OATP substrates, are eliminated from the liver by metabolism and/or biliary excretion, while small and hydrophilic organic anions, such as OAT substrates, are excreted into the urine. The tissue distribution and elimination pathways of drugs can be explained by similarities and differences in the substrate recognition by these transporters expressed in the liver and kidney. Thus, modifying the drug so that it is recognized by OATP or OAT may lead to liver or kidney organotropism. Although, in general, OAT families are mainly expressed in the kidney, OAT2 is abundantly expressed in the liver and, to a lesser extent, in the kidney, and localized to the basolateral membrane of the liver (Simonson et al., 1994; Sekine et al., 1998). OAT2 transports relatively small and hydrophilic organic anions, such as indomethacin and salicylate, and may be involved in the hepatic uptake of these drugs (Morita et al., 2001). However, the OATP family is supposed to be responsible for the hepatic uptake of amphipathic organic anions.

The reported toxicity of some drugs is occasionally caused by concentrative tissue distribution due to active transport. The OAT1-mediated transport of ochratoxin A, a potent nephrotoxin, has been reported, suggesting that accumulation of the toxin via OAT1 in proximal tubules may be the primary event in the development of ochratoxin A-induced nephrotoxicity (Tsuda et al., 1999; Jung et al., 2001b). A similar effect has been proposed for adefovir, cephalosporin antibiotics, and β-lactam antibiotics, which accumulate extensively in the tubules (Cihlar et al., 1999; Jariyawat et al., 1999; Takeda et al., 1999, 2002a). Active transport processes may increase the intracellular concentration and appear to be directly related the development of tubular injury. Thus, designing a drug that is not transported by OAT1 or coadministering OAT1 inhibitors may be an effective way of reducing the nephrotoxicity of these compounds (Cihlar et al., 2001). A fluorescence assay to screen for novel human OAT1 inhibitors has been developed (Cihlar and Ho, 2000) and it has been suggested that NSAIDs may reduce adefovir nephrotoxicity since they efficiently inhibit the human OAT1-specific transport of adefovir at clinically relevant concentrations (Apiwattanakul et al., 1999; Mulato et al., 2000).

3. Organic Cation Transporter (SLC22A) Family. The OCT family of proteins is involved in the uptake of organic cations into the liver or kidney from blood. OCT1 and OCT2 are expressed in epithelial cells of the kidney, liver, and intestine, and appear to be localized to the basolateral membranes of the cells (Table 1) (Meyer-Wentrup et al., 1998; Urakami et al., 1998). These transporters mediate the uptake of a variety of organic cations, such as dopamine, choline, 1-methyl-4-phenylpyridinium (MPP^+), N^1-methylnicotinamide, TEA, and cimetidine (Martel et al., 1996; Zhang et al., 1997; Breidert et al., 1998; Koepsell, 1998; Urakami et al., 1998; Zhang et al., 1998). Rat Oct1 is expressed in both the liver and kidney, although its human counterpart is expressed predominantly in the liver, while human and rat Oct2 are present mainly in kidney and brain (Grundemann et al., 1994; Gorboulev et al., 1997). Rat Oct3 mRNA has been found to be most abundant in the placenta, with a moderate presence in the intestine, heart, and brain (Kekuda et al., 1998).

Recently, the pharmacological and physiologic role of Oct1 has been investigated using Oct1 knockout (Oct1$^{-/-}$) mice (Jonker et al., 2001). The distribution and excretion of the model substrate TEA after intravenous administration has been compared in wild-type and Oct1$^{-/-}$ mice. In Oct1$^{-/-}$ mice, accumulation of TEA in liver was 4- to 6-fold lower than in wild-type mice, indicating that for TEA, Oct1 is the main uptake system in the liver (Table 7). In addition, direct intestinal excretion of TEA was reduced about 2-fold, showing that Oct1 also mediates basolateral uptake of TEA into enterocytes (Table 7). Excretion of TEA into urine over 1 h accounted for 53% of the dose in wild-type mice compared with 80% in knockout mice, probably because in Oct1$^{-/-}$ mice less TEA accumulates in the liver and thus more is available for rapid excretion by the kidney (Table 7).

Similarly, the distribution of metformin, a biguanide, to the liver and intestine in Oct1$^{-/-}$ mice was significantly lower than that in wild-type mice, whereas distribution to the kidney and the urinary excretion profile showed only minimal differences (Wang et al., 2002). Oct1 is responsible for hepatic uptake as well as playing a role in the intestinal uptake (via basolateral membrane) of metformin, while the renal distribution and excretion are mainly governed by other transport mechanisms. Biguanides are oral antihyperglycemic agents used for the treatment of type 2 diabetes mellitus, but they are associated with lactic acidosis, a potentially fatal side effect. Following the administration of metformin, the blood lactate concentration significantly increased in wild-type mice, whereas only a slight increase was observed in Oct1$^{-/-}$ mice (Wang et al., 2003). The hepatic concentration of metformin in Oct1$^{-/-}$ mice was markedly reduced, whereas its plasma concentration time profile was similar in wild-type and Oct1$^{-/-}$ mice. These results indicate that the Oct1-mediated hepatic uptake of biguanides plays an important role in lactic acidosis.

TABLE 7

Levels of radioactivity in female wild-type and Oct1$^{-/-}$ mice with a cannulated gallbladder at 60 min after i.v. injection of [^{14}C]TEA (0.2 mg/kg) (Jonker et al., 2001)

	^{14}C concn (ng-eq g^{-1} or ml^{-1}) ± SD (n = 4)		Excretion (%)[c]		Ratio (Oct1$^{-/-}$/wt)
	wt[a]	Oct1$^{-/-}$	wt	Oct1$^{-/-}$	
Plasma	23.8 ± 4.9	17.1 ± 3.0*			0.72
Brain	1.6 ± 0.3	1.9 ± 0.4			1.22
Spleen	35 ± 5	42 ± 2*			1.21
Kidney	441 ± 152	236 ± 20*			0.53
Liver	1225 ± 26 (25.3±0.8[b])	283 ± 44**(5.8±1.0**)			0.23
Bile			0.35 ± 0.09	0.14 ± 0.01*	0.41
Small intestine			1.31 ± 0.19	0.67 ± 0.09**	0.51
Cecum			0.12 ± 0.02	0.09 ± 0.04*	0.72
Colon			0.03 ± 0.01	0.04 ± 0.01	1.23
Urine			53.3 ± 16.8	80.0 ± 15.6*	1.50

* $P < 0.05$; ** $P < 0.01$.
[a] wt, wild type.
[b] Mean percentage of administered dose ± SD (n = 4).
[c] Total TEA found in the contents of small intestine, cecum, and colon. Urine was collected from the bladder.

4. Multidrug Resistance-Associated Protein 2 (ABCC2). MRP2, located on the bile canalicular membrane, is involved in the biliary excretion of clinically important anionic drugs as well as the intracellularly formed glucuronide- and glutathione-conjugates of many drugs (Paulusma et al., 1996; Ito et al., 1997; Keppler et al., 1997; Ito et al., 1998b; Konig et al., 1999a). In the liver, xenobiotics are metabolized by the so-called phase I and II enzymes, which are mainly cytochrome P450 and conjugating enzymes, respectively. After these enzymatic reactions, the conjugated metabolites produced are pumped out from hepatocytes into the bile. This ATP-dependent efflux transporter plays a physiologically important role as the "phase III" xenobiotic detoxification system (Ishikawa, 1992). In addition, MRP2 mediates the biliary excretion of not only conjugated metabolites, but also unchanged organic anions, such as grepafloxacin (a new fluoroquinolone antibiotics) or cefodizime and ceftriaxone (β-lactam antibiotics) (Sathirakul et al., 1993; Kusuhara et al., 1998; Sasabe et al., 1998). These antibiotics have been shown to be effective in the treatment of inflammatory conditions affecting the biliary tract because they are efficiently excreted into the bile (Suzuki and Sugiyama, 1999). The biliary excretion of these antibiotics gives these drugs a pharmacological advantage due to the target organ.

However, in some cases there is a major accumulation of drugs in the bile duct via MRP2 expressed on the bile canalicular membrane, which results in toxic effects on bile epithelial cells or gastrointestinal cells. It is supposed that the reactive glucuronide of the NSAID diclofenac is selectively transported into bile via MRP2, where it exhibits toxic effects on the bile canalicular membrane (Seitz et al., 1998). Similarly, methotrexate is concentrated in bile compared with plasma and undergoes enterohepatic circulation, resulting in adverse effects in the intestine. It has been reported that the biliary excretion of methotrexate is mediated by MRP2 (Masuda et al., 1997). A structural modification of such drugs to reduce their biliary excretion would be useful.

Although CPT-11 is an effective anticancer drug, its clinical use is frequently limited by a form of gastrointestinal toxicity, severe diarrhea (Rowinsky et al., 1994). Such severe diarrhea exhibits a large degree of interpatient variability. The action of its active metabolite, SN-38, on gastrointestinal cells is believed to be responsible for this toxicity (Araki et al., 1993). The biliary excretion of SN-38 and SN-38 glucuronide and subsequent uptake by gastrointestinal epithelial cells may be associated with this diarrhea (Kaneda and Yokokura, 1990). It has been shown that MRP2 is involved in the biliary excretion of SN-38 and SN-38 glucuronide (Chu et al., 1997a,b), and there is a large degree of interindividual variability in the transport activity of SN-38 via MRP2, as shown by a study using human bile canalicular membrane vesicles (CMVs) (Chu et al., 1998). Thus, the biliary excretion of its metabolites mediated by MRP2 has been proposed to be linked to its unpredictable gastrointestinal toxicity. An attempt to prevent this toxicity using potent MRP2 inhibitors has been investigated. Probenecid is a potential candidate, which can be used clinically to inhibit the biliary excretion of CPT-11 metabolites (Horikawa et al., 2002b). In actual fact, it has been shown that coadministration of probenecid markedly reduces both SN-38 exposure and CPT-11-induced late-onset toxicity in the gastrointestinal tissues of rats, possibly by inhibiting the biliary excretion of CPT-11 and/or its metabolites (Horikawa et al., 2002a). It is expected that this agent will be used clinically to prevent toxicity. Approaches using intentional drug-drug interactions (positive drug interactions) like this case may become more important in the future.

Control of the elimination route, such as biliary or urinary excretion, is also one of the strategies used to avoid potentially toxic effects. In some cases, transporters expressed in the liver or kidney may determine the elimination route affecting the systemic plasma concentrations of drugs. Many ACE inhibitors are actually administered as prodrugs and are metabolized to their active forms, such as enalaprilat, captoprilat, cilazaprilat, ramiprilat, and spirapprilat. They are excreted predominantly into the urine. In contrast, temocaprilat is excreted via both bile and urine (Oguchi et al., 1993).

The presence of an excretion route other than the urinary one confers a pharmacokinetic advantage, particularly in the treatment of patients with renal failure. In such patients, the AUC and C_{max} values of captopril and enalapril are markedly increased because these ACE inhibitors are eliminated primarily via renal excretion (Oguchi et al., 1993). In contrast, alterations in these pharmacokinetic parameters are minimal for temocaprilat because of the presence of the biliary excretion pathway (Oguchi et al., 1993). A multiple elimination pathway will result in a relatively stable pharmacokinetic profile compared with only a single elimination pathway. Although the biliary excretion of temocaprilat is governed by MRP2 at the canalicular membrane, it has been suggested that other ACE inhibitors are not good substrates of MRP2 (Ishizuka et al., 1997, 1999). The affinity for MRP2 is expected to be the predominant factor in determining the biliary excretion of any series of ACE inhibitors. Drugs that are excreted into both the bile and urine to the same degree may be expected to exhibit minimal interindividual differences in their pharmacokinetics.

Mrp2-deficient rats, such as transport-deficient rats and Eisai hyperbilirubinemic rats, exhibit hyperbilirubinemia such as the Dubin-Johnson syndrome due to a defect in the biliary excretion of bilirubin glucuronides. Mrp3 is induced on the hepatic basolateral membrane of Mrp2-deficient animals (Hirohashi et al., 1998; Donner and Keppler, 2001; Soroka et al., 2001) and is able to excrete glucuronide conjugates of xenobiotics (Hirohashi et al., 1999, 2000b). Thus, these results are consistent with the hypothesis that Mrp3 may be involved in the sinusoidal efflux of glucuronide conjugates in these mutants. It is plausible that in the cholestatic liver, bilirubin glucuronides are effluxed from the liver into the blood via sinusoidal Mrp3, resulting in jaundice. Moreover, immunohistochemical studies have indicated that MRP3 is induced in the sinusoidal membrane of patients suffering from Dubin-Johnson syndrome (Konig et al., 1999b).

5. Bile Salt Export Pump (ABCB11). Intrahepatic cholestasis can be induced by interference with the secretion of biliary constituents resulting in an intracellular accumulation of bile salts and other toxic bile constituents within hepatocytes. BSEP, located on the canalicular membrane, mediates the transport of bile acids such as taurocholic acid (Gerloff et al., 1998; Kullak-Ublick et al., 2000). Cholestasis induced by some drugs is mediated, at least in part, by inhibition of BSEP, resulting in intracellular accumulation of cytotoxic bile salts. The immunosuppressant, cyclosporine, has been shown to produce *cis*-inhibition of BSEP-mediated bile salt transport (Stieger et al., 2000). A similar mechanism has been postulated for rifampicin and glibenclamide (Stieger et al., 2000). In contrast, the cholestatic estrogen metabolite, E_2-17βG, causes *trans*-inhibition of BSEP-mediated bile salt transport and, therefore, exerts its cholestatic action only after its excretion by MRP2 into the canalicular lumen (Stieger et al., 2000). In addition, some other MRP2 substrates cause *trans*-inhibition of the BSEP-mediated transport of bile acids (Akita et al., 2001). Horikawa et al. have reported the inhibition potential of a series of therapeutic drugs, producing clinical cholestasis, on BSEP and MRP2 (Horikawa et al., 2003). Although most of the drugs have only a minimal inhibitory effect on Bsep- and Mrp2-mediated transport in rat CMVs, cloxacillin inhibited BSEP-mediated transport in both rat and human CMVs. Since the inhibitory effect on BSEP-mediated transport by cloxacillin was more marked in human CMVs than in rat CMVs, species differences in inhibitory potential need to be considered (Horikawa et al., 2003). Troglitazone is a thiazolidinedione insulin-sensitizing agent for the treatment of noninsulin-dependent diabetes mellitus, but it was withdrawn from the market because of liver toxicity (Funk et al., 2001a). Although the mechanism underlying this troglitazone-associated hepatotoxicity is at present unclear, it has been suggested that a cholestatic mechanism is involved (Funk et al., 2001a). Troglitazone and, to a much greater extent troglitazone sulfate, the main troglitazone metabolite eliminated into bile, competitively inhibit ATP-dependent taurocholate transport via BSEP (Funk et al., 2001a,b). This inhibition of the hepatobiliary export of bile salts by troglitazone and troglitazone sulfate may lead to a drug-induced intrahepatic cholestasis in humans, possibly contributing to the hepatotoxicity of troglitazone. One should consider the possibility that drugs which inhibit BSEP may cause cholestasis. The evaluation of BSEP inhibition will play an important role in the identification of compounds that could be a potential cause of cholestasis.

Obtaining more data on the substrate specificities and expression level of each human transporter will be of great help in improving drug design by targeting specific transporters and controlling their elimination. The route of elimination may be controlled by using transporters that are expressed selectively in either the liver or kidney.

III. Clinical Implications of Transporter-Mediated Drug Interactions

A. Drug-Drug Interactions Involving Elimination

Drug-drug interactions involving membrane transport can be classified into two categories: one caused by competition for the substrate binding sites of the transporters, and the other caused by a change in the expression level of the transporters. Due to the broad substrate specificity of P-gp, drug-drug interactions involving P-gp are very likely (Lin, 2003). Table 8 gives an overview of the known drug interactions that involve, at least in part, P-gp. This gives an indication of the interactions that one may expect during combination therapy. P-gp

TABLE 8
Example of the possible involvement of P-gp with clinical drug-drug interactions

Inhibitor or Inducer				Inhibited or Induced Drug							Possible Mechanisms of Drug-Drug Interactions	Reference
	IC_{50} or K_i in vitro (μM)[a]		Dose (mg)		AUC	C_{max}	BA	CL	$T_{1/2}$	Others		
	Mean	Range[b]			*-fold*							
Inhibition												
Valspodar	0.182	0.022–0.41	400	Digoxin				CL_r −62%			A	Kovarik et al., 1999
				Paclitaxel	2.5							Sikic et al., 2000
			400	Dexamethasone	1.24							Kovarik et al., 1998
Erythromycin	105	10–200	500	Atrovastatin	1.32	1.38			NS		B	Siedlik et al., 1999
			1500	Digoxin		2.04					A	Maxwell et al., 1989
			2000	Talinolol	1.34				NS		A	Schwarz et al., 2000
				Fexofenadine	2.09	1.82					A	Davit et al., 1999
			1000	Saquinavir	1.99	2.06					B	Grub et al., 2001
			1000	Cyclosporine	1.97	2.13		CL −38%	NS	Met% in plasma −49%	B	Freeman et al., 1987
			2000	Cyclosporine	2.15	2.8	36→60%		NS		B	Gupta et al., 1988
			2000	Cyclosporine	2.15		36→60%	CL −13%			B	Gupta et al., 1989
Verapamil	83.1	3–236	240	Digoxin		1.44		CL_{bile} −43%, CL_r, NS			A	Hedman et al., 1991
			160	Digoxin		1.4					A	Mackstaller and Alpert, 1997
			240	Digoxin		1.6–1.8					A	Cobbe, 1997
Itraconazole			200	Digoxin	1.5			CL_r −20%			A	Jalava et al., 1997
			200	Quinidine	2.4	1.6		CL_r −50%	×1.6	M/P(AUC) −50%	B	Kaukonen et al., 1997
Cyclosporine	7.24	3.4–17	1050	Docetaxel	11.2		8→90%				B	Malingre et al., 2001b
			1050	Paclitaxel	8			×8			B	Meerum Terwogt et al., 1999
			180–540	Paclitaxel	1	1						Britten et al., 2000
			280	Sirolimus	1.45	1.71					B	Kaplan et al., 1998
			16 mg/kg infusion	Doxorubicin	1.8			CL −37%	NS	M/P(AUC) −75%	B	Rushing et al., 1994
			5–21 mg/kg	Etoposide	1.59			CL_{tot} −35%	×1.73			Lum et al., 1992
GF120918			1000	Paclitaxel	7		×7				B	Malingre et al., 2001a
			800	Doxorubicin	1			CL_r NS				Sparreboom et al., 1999
Quinidine	62.8	1.5–157		Digoxin		2		CL_{tot} −50%			A	Yu, 1999
			800	Digoxin		1.54		CL_{bile} −42%, CL_r −29%			A	Hedman et al., 1990
Quinine	280		750	Digoxin		1.1		CL_{bile} −35%			A	Hedman et al., 1990
Ketoconazole	18.8	1.5–36		Fexofenadine	2.64	2.35					A	Davit et al., 1999
			400	Saquinavir	2.9	2.71					B	Grub et al., 2001
			200	Saquinavir	1.69	1.36					B	Grub et al., 2001
			200	Tacrolimus	2		14→30%	CL, F_h, NS			B	Floren et al., 1997

TABLE 8
Continued

Inhibitor or Inducer			Inhibited or Induced Drug								
IC_{50} or K_i in vitro (μM)[a]		Dose (mg)		AUC	C_{max}	BA	CL	$T_{1/2}$	Others	Possible Mechanisms of Drug-Drug Interactions	Reference
Mean	Range[b]										
Propafenone		600	Digoxin	*-fold*			CL_{tot} −31%, CL_r −32%			A	Calvo et al., 1989
Clarithromycin			Digoxin				CL_r −48%			A	Wakasugi et al., 1998
Vitamin E			Cyclosporine	1.61	1.37				M/P(AUC) NS	C	Chang et al., 1996
Talinolol		100	Digoxin	1.23	1.45		CL_r NS	NS		A	Westphal et al., 2000a
Ritonavir		300	Saquinavir	58	33					B	Merry et al., 1997
Nelfinavir		2250	Azithromycin	2	2						Amsden et al., 2000
Diltiazem		30	Tacrolimus		4.3					B	Hebert and Lam, 1999
Atrovastatin		80	Digoxin	1.15	1.2					A	Boyd et al., 2000
		10	Digoxin		1						Boyd et al., 2000
Induction											
Rifampin		600	Fexofenadine	0.43	0.59		CL_r NS	NS		A	Hamman et al., 2001
		600	Talinolol	0.65			P-gp ×4.2			A	Westphal et al., 2000b
		600	Tacrolimus			14→7%	CL_{tot} +47%				Hebert et al., 1999
		600	Digoxin	0.42			CL_r NS	NS	P-gp ×3.5	A	Greiner et al., 1999
		600	Glyburide	0.78				−15%		C	Niemi et al., 2001
		600	Glipizide					−36%		C	Niemi et al., 2001
		600	Saquinavir	0.35							Grub et al., 2001
		600	Saquinavir	0.57							Grub et al., 2001
St. John's wort			Digoxin	0.82					P-gp ×1.4	A	Durr et al., 2000
			Digoxin	0.75	0.74					A	Johne et al., 1999
			Cyclosporine	Trough conc. −64%							Barone et al., 2000

BA, bioavailability; CL_r, renal clearance; CL_{tot}, total clearance; CL_{bile}, biliary clearance; NS, not significant; M/P(AUC), the ratio of AUC of metabolites to that of parent drugs; A, involvement of P-gp is suggested to be obvious; B, the cases cannot be distinguished between involvement of P-gp and CYP3A4; C, the cases cannot discriminate among other possibilities.

[a] IC_{50} or K_i values in vitro are cited from Wu et al., 2000; Kim et al., 1999; Kawahara et al., 2000; Zhang and Benet, 1998; Yumoto et al., 1999; Gao et al., 2001; Tiberghien and Loor, 1996.

[b] Represents minimal and maximal values reported by several authors.

inhibitors, such as quinidine, valspodar, and verapamil, are known to increase plasma concentrations of digoxin, a cardiac glycoside, because they block its biliary and/or urinary excretion via P-gp (Table 8) (Hedman et al., 1990, 1991; Kovarik et al., 1999). Since the therapeutic range of digoxin is small, changes in its plasma concentration are potentially very serious.

Since OAT1 is responsible for the urinary excretion of a wide variety of anionic agents, it may be involved in renal drug-drug interactions. Furosemide undergoes tubular secretion before reaching its target site, the loop of Henle. Coadministration of probenecid significantly inhibits the tubular secretion of furosemide and, therefore, its diuretic effect is markedly reduced (Inui et al., 2000a; Uwai et al., 2000). It is well known that probenecid inhibits the renal secretion of many other anionic drugs via organic anion transport systems. The renal excretion of ciprofloxacin, benzylpenicillin, and acyclovir is reduced by coadministration of probenecid (Overbosch et al., 1988; Tsuji et al., 1990; Jaehde et al., 1995). OAT1 is a candidate for the transporter responsible for these interactions on the renal basolateral membrane because probenecid is able to inhibit OAT1 (Hosoyamada et al., 1999). In addition, fatal interactions have been reported between methotrexate and NSAIDs (Tracy et al., 1992; Kremer and Hamilton, 1995). NSAIDs significantly reduced methotrexate renal clearance This interaction seems to be linked to severe adverse effects after chemotherapy (Thyss et al., 1986). Methotrexate is specifically taken up by OAT1- or OAT3-expressing cells, and NSAIDs inhibit the methotrexate uptake mediated by these transporters (Takeda et al., 2002b). These results suggest that the basolateral membrane OAT1 and/or OAT3 is involved in the methotrexate-NSAID interaction in the kidney.

In addition, hepatic drug-drug interaction via OATP-C has been reported. In kidney transplant recipients treated with cyclosporine, the AUC of cerivastatin was 3.8-fold higher than that in healthy volunteers who were not given cyclosporine (Fig. 3) (Muck et al., 1999). The mild-to-moderate reduction in renal function in kidney transplant recipients compared with healthy controls is unlikely to be responsible for the observed pharmacokinetic effects, because the renal clearance of cerivastatin is negligible (Muck et al., 1997). Shitara et al. have examined the effect of cyclosporine on the uptake of cerivastatin into human hepatocytes to investigate the mechanism of their drug-drug interaction (Shitara et al., 2003). As a result, cyclosporine was found to inhibit transporter-mediated cerivastatin uptake in human hepatocytes with K_i values of 0.28 to 0.69 μM. In addition, the uptake of cerivastatin was examined in human OATP-C-expressing MDCK II cells and cerivastatin was shown to be a substrate of human OATP-C, like pravastatin (Hsiang et al., 1999; Nakai et al., 2001). OATP-C-mediated uptake of cerivastatin was also inhibited by cyclosporine with a K_i value of 0.2 μM in transfected cells. These results suggest that the drug-drug interaction between cerivastatin and cyclosporine can be explained by inhibition of the transporter-mediated hepatic uptake of cerivastatin and, at least in part, its OATP-C-mediated uptake. Recently, a severe drug-drug interaction between cerivastatin and gemfibrozil was reported and, in the United States, 31 deaths from severe rhabdomyolysis were reported in patients taking cerivastatin, 12 of whom were taking concomitant gemfibrozil (Charatan, 2001). This resulted in the withdrawal of cerivastatin from the market (Alexandridis et al., 2000; SoRelle, 2001). It is possible that the transporter in the sinusoidal membrane of the liver is involved in this drug-drug interaction, and the mechanism governing this needs to be investigated.

B. Drug-Drug Interactions Involving Absorption

There are some instances where intestinal P-gp may be involved in human drug-drug interactions associated with absorption (Table 8). For example, coadministration of erythromycin, a macrolide antibiotic, enhances the AUC of the orally administered β-blocker, talinolol, by 34% (Schwarz et al., 2000). A P-gp substrate, talinolol is eliminated mainly via the urine without any significant systemic metabolism. The renal clearance of talinolol is unaffected by coadministration of erythromycin, hence its intestinal absorption appears to be altered by coadministration of erythromycin (Schwarz et al., 2000). Therefore, it appears that the increase in oral bioavailability of talinolol after concomitant administration of erythromycin is caused by an increased net intestinal absorption due to P-gp inhibition by the latter. The metabolism by CYP3A in the human small intestine is a major factor limiting oral bioavailability, accompanied by P-gp-mediated efflux (Wacher et al., 2001; Zhang and Benet, 2001). Talinolol or digoxin is a good substrate of P-gp, but not of CYP3A. Thus, the role of P-gp in intestinal secretion is directly confirmed by these examples. Since the substrate specificities of CYP3A and P-gp overlap (Wacher et al., 1995), many drugs may be substrates of both. In such cases it is difficult to distinguish between the contribution of CYP3A and that of P-gp to the increased oral bioavailability.

Recently, an interesting report has appeared describing an interaction between fexofenadine and grapefruit, orange, and apple juice (Dresser et al., 2002). Unmetabolized fexofenadine is a substrate of P-gp, and it is known that grapefruit juice may inhibit P-gp activity (Spahn-Langguth and Langguth, 2001). Thus, it can be predicted that the plasma concentration of orally administered fexofenadine will be increased by coadministration of grapefruit juice if the latter inhibits intestinal P-gp. Nevertheless, grapefruit juice produced markedly lower plasma fexofenadine concentrations in healthy volunteers (Table 9) (Dresser et al., 2002). The fexofenadine AUC and C_{max} values following the administration of grapefruit juice were reduced to approximately 30% of

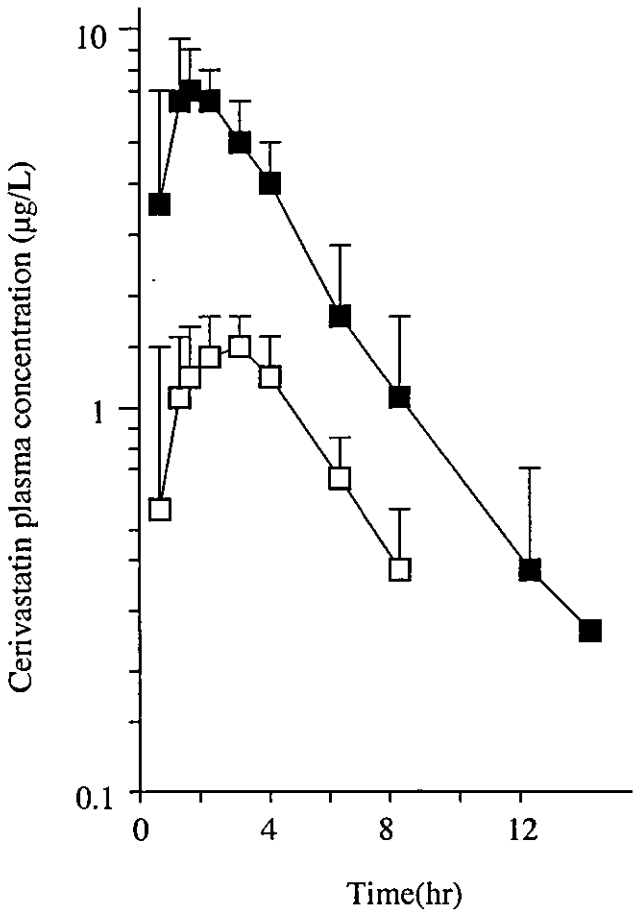

FIG. 3. Change in the disposition of cerivastatin caused by cyclosporine treatment. Cerivastatin plasma concentration-time profiles after oral administration of 0.2 mg cerivastatin in kidney transplant recipients receiving stable individual cyclosporine treatment (■) compared with healthy subjects without cyclosporine intake (□) are shown (Muck et al., 1999).

those following administration of water, while the fexofenadine elimination half-life and renal clearance remained unaffected. Similar phenomena have been reported following the coadministration of orange or apple juice. Fexofenadine is actually the substrate of not only P-gp, but also the drug uptake transporter, OATP (Cvetkovic et al., 1999). In addition, grapefruit juice produces a modest inhibition of P-gp-mediated digoxin efflux transport in cell lines expressing P-gp. In contrast, grapefruit, orange, and apple juices caused marked inhibition of OATP-mediated fexofenadine uptake in cell lines expressing OATPs. In view of the above results, it appears that OATP-mediated fexofenadine uptake is actually inhibited. Since inhibition of P-gp and OATPs in the liver would reduce the biliary secretion and increase plasma fexofenadine concentrations, it appears that the fexofenadine-juice interaction is primarily the result of reduced fexofenadine absorption from the gastrointestinal tract. Fruit juices are more potent inhibitors of OATPs than P-gp, which can reduce oral drug bioavailability.

Induction of transporter represents a new type of drug-drug interaction. Greiner et al. have reported a rifampin-digoxin interaction involving the induction of intestinal P-gp in humans (Greiner et al., 1999). The AUC value of oral digoxin is significantly lower during rifampicin treatment (600 mg/day for 10 days) but the effect is less pronounced after intravenous administration of digoxin (Greiner et al., 1999) (Table 10). The renal clearance and half-life of digoxin are unaltered by rifampin. However, rifampin treatment increases the intestinal P-gp content 3.5-fold, which correlates with the AUC value after oral but not intravenous administration of digoxin (Fig. 4). P-gp is a determinant of the disposition of digoxin and the rifampin-digoxin interaction appears to occur largely at the level of the intestinal P-gp expression. Since rifampin also induces intestinal MRP2, coadministration of rifampin is expected to increase the secretion into the lumen of MRP2 substrates, such as glutathione or glucuronide conjugates (Fromm et al., 2000). St. John's wort is one of the most commonly used over-the-counter herbal medicines in the United States and is widely used in the treatment of mild depression. However, the U.S. Food and Drug Administration alerted health professionals to the risk of drug interactions with St. John's wort (Henney, 2000). Coadministration of St. John's wort and the HIV protease inhibitor indinavir reduced the latter's exposure by 57% in healthy volunteers (Piscitelli et al., 2000). The induction of intestinal P-gp by St. John's wort is assumed to play a role in these phenomena. In addition, the administration of St. John's wort to healthy volunteers over 14 days resulted in an 18% reduction in digoxin exposure after a single dose of digoxin, and a 1.4- and 1.5-fold increase in the expression of duodenal P-gp and CYP3A4, respectively (Table 8) (Durr et al., 2000). Although St. John's wort induces both P-gp and CYP3A4, like rifampin, the reduction in the oral bioavailability of digoxin may be caused by the induction of

TABLE 9
Reduction of fexofenadine bioavailability by fruit juices in humans (Dresser et al., 2002)

	Control	Grapefruit Juice	Orange Juice	Apple Juice
$AUC_{(0-8h)}$ (ng · h/ml)	1330 ± 109	439 ± 44*	373 ± 19*	301 ± 33*
C_{max} (ng/ml)	288 ± 23	110 ± 14*	96 ± 7*	81 ± 13*
$T_{1/2}$ (h)	2.6 ± 0.2	3.1 ± 0.2	3.4 ± 0.3	3.5 ± 0.4
CL_r (ml/min)	78 ± 8	74 ± 7	86 ± 8	92 ± 9

Fexofenadine 120 mg with 1200 ml of water, grapefruit juice, orange juice, or apple juice was administered to 10 healthy volunteers. Data are expressed as mean ± S.E.M. Comparisons are between juice and water treatments.
* $P < 0.001$.

TABLE 10
The effect of rifampin on pharmacokinetics of digoxin in humans (Greiner et al., 1999)

	Digoxin 1 mg p.o.		Digoxin 1 mg i.v.	
	Control	With Rifampin[a]	Control	With Rifampin[a]
$AUC_{(0-144h)}$ (ng/h/ml)	54.8 ± 11.6	38.2 ± 12.4*	87.3 ± 8.3	74.5 ± 10.5*
Bioavailability (%)	63 ± 11	44 ± 14*		
T_{max} (min)	42 ± 12	52 ± 18*		
C_{max} (ng/ml)	5.4 ± 1.9	2.6 ± 0.7**	24.7 ± 5.2	20.9 ± 1.8
Renal clearance (ml/min)	159 ± 30	159 ± 38	151 ± 25	147 ± 18
Nonrenal clearance (ml/min)			17 ± 17	54 ± 29**
$T_{1/2}$ (h)	56 ± 13	54 ± 13	58 ± 12	53 ± 11

[a] 600 mg/day of rifampin were administered to healthy volunteers for 10 days.
* $P < 0.05$; ** $P < 0.01$.

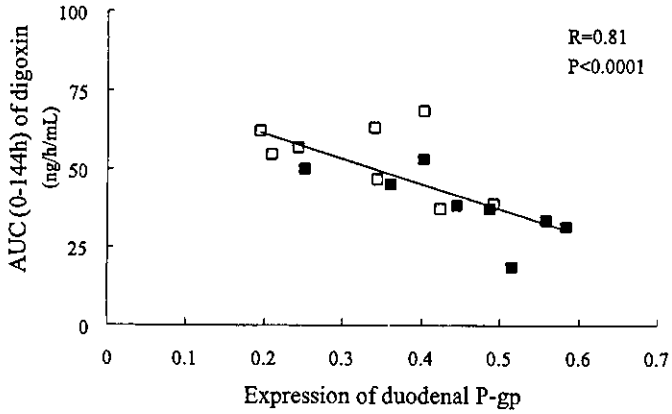

FIG. 4. Correlation between AUC of orally administrated digoxin (1 mg) and expression of duodenal P-gp in humans (n = 16). □, without rifampin; ■, with rifampin (600 mg) (Greiner et al., 1999).

intestinal P-gp due to a lack of significant metabolism by CYP3A4.

C. Prediction of in Vivo Drug-Drug Interactions from in Vitro Data

Although remarkable progress has been made in the identification and functional characterization of drug transporters, quantitative evaluation of drug-drug interactions involving the membrane transport process is difficult compared with that of drug-drug interactions involving metabolism. Overall, interactions involving membrane transporters in organs of elimination (e.g., liver and kidney) and absorption (e.g., intestine) alter the blood concentration-time profiles of drugs. In contrast, interactions occurring at the blood-brain barrier and in tumors will not alter the drug exposure in the circulating blood, only the pharmacological and/or toxicological effect of the drugs involved. Although there is not much difference between mdr1a knockout mice and wild-type mice as far as the plasma concentrations of many drugs are concerned, the brain concentrations are markedly increased in mdr1a knockout mice, as shown in Table 4. Evaluating the change in plasma drug concentrations alone is not enough to study drug-drug interactions involving the membrane transport process, and changes in the tissue distribution of drugs should also be taken into consideration.

Ito et al. (1998a) have previously proposed a method for predicting in vivo drug-drug interactions involving hepatic metabolism from in vitro experiments. A similar method can be used to predict in vivo drug-drug interactions involving biliary excretion (Kusuhara and Sugiyama, 2001a). Assuming that the contribution of passive diffusion to the membrane transport process is negligible, the reduction in intrinsic membrane transport clearance (PS_{int}) produced by an inhibitor can be predicted from eq. 1 of Fig. 5 (Ito et al., 1998a): where I_u and K_i represent the unbound concentration of an inhibitor around a transporter and its inhibition constant, respectively. When the substrate concentration is much lower than the K_m value (this assumption holds true for many drugs at their clinical dosages), the degree of inhibition (R) is defined by eq. 1 of Fig. 5, independent of the type of inhibition (Ito et al., 1998a). Compared with drug interactions involving hepatic metabolism, the prediction of biliary excretion is a more complicated procedure because at least three membrane transport processes have to be considered to successfully predict the excretion. The intrinsic clearance for the net biliary excretion from the blood ($CL_{int,bile}$) is a hybrid of the intrinsic clearances for each membrane penetration: hepatic uptake across the sinusoidal membrane (PS_1), efflux across the sinusoidal membrane from the liver (PS_2), and excretion across the canalicular membrane (PS_3), as shown in eq. 4 of Fig. 5. Thus, one can predict a drug interaction involving each type of membrane transport separately based on the Michaelis-Menten equation (eq. 1 of Fig. 5). To demonstrate the validity of the prediction method based on these equations, Ueda et al. attempted to predict the interaction between methotrexate and probenecid involving biliary excretion in rats using in vitro systems (Ueda et al., 2001). This interaction has already been reported in a clinical situation. Coadministration of probenecid reduced the biliary clearance of methotrexate in rats. This inhibition by probenecid was confirmed in vivo for both the uptake and excretion processes of methotrexate across the sinusoidal and canalicular membranes, respectively. Both the hepatic uptake clearance (PS_1), assessed by integration plot analysis, and the steady-state biliary clearance

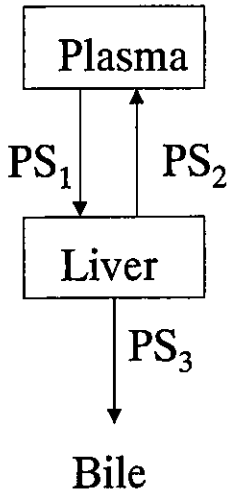

$$R = \frac{PS_{int}(+inhibitor)}{PS_{int}(control)} = \frac{1}{1 + I_u / K_i} \quad \text{(Eq. 1)}$$

$$R_{uptake} = \frac{PS_1(+inhibitor)}{PS_1(control)} = \frac{1}{1 + I_{u,plasma} / K_{i,1}} \quad \text{(Eq. 2)}$$

$$R_{excretion} = \frac{PS_3(+inhibitor)}{PS_3(control)} = \frac{1}{1 + I_{u,liver} / K_{i,3}} \quad \text{(Eq. 3)}$$

$$CL_{int,bile} = PS_1 \times \frac{PS_3}{PS_2 + PS_3} \quad \text{(Eq. 4)}$$

$$R = \frac{CL_{int,bile}(+inhibitor)}{CL_{int,bile}(control)} \leqq R_{uptake} \times R_{excretion} \quad \text{(Eq. 5)}$$

FIG. 5. Schematic diagram illustrating the model of biliary excretion considering each processes of membrane penetration. PS_{int} represents the intrinsic membrane transport clearance. I_u and K_i represent the unbound concentration of an inhibitor around a transporter and its inhibition constant, respectively. PS_1, PS_2, and PS_3 represent the intrinsic membrane transport clearance for hepatic uptake across the sinusoidal membrane, that for efflux across the sinusoidal membrane from the liver, and that for excretion across the canalicular membrane, respectively. $I_{u,plasma}$ and $I_{u,liver}$ represent the unbound concentration of an inhibitor in plasma and that in liver, respectively. $K_{i,1}$ and $K_{i,3}$ represent the inhibition constant of an inhibitor for a hepatic uptake process across the sinusoidal membrane and that for an excretion process across the canalicular membrane, respectively. $CL_{int,bile}$ represents the intrinsic clearance for the net biliary excretion from the blood.

(PS_3) defined with respect to the hepatic unbound methotrexate, were reduced in the presence of probenecid in vivo. Furthermore, to predict drug interactions associated with membrane transport via sinusoidal and canalicular membranes from in vitro data using eqs. 2 and 3 of Fig. 5, $K_{i,1}$ and $K_{i,3}$ values were obtained in isolated hepatocytes and CMVs, respectively. The unbound concentration of the inhibitor ($I_{u,plasma}$ and $I_{u,liver}$) was directly estimated both in plasma and liver in vivo. As a result, the degree of inhibition of the uptake (PS_1) and excretion (PS_3) processes found in vivo was comparable with the predicted values using the inhibition constant obtained using isolated hepatocytes and CMVs, respectively (Fig. 6). This suggests that the interaction associated with each membrane transport process can be quantitatively estimated from in vitro data.

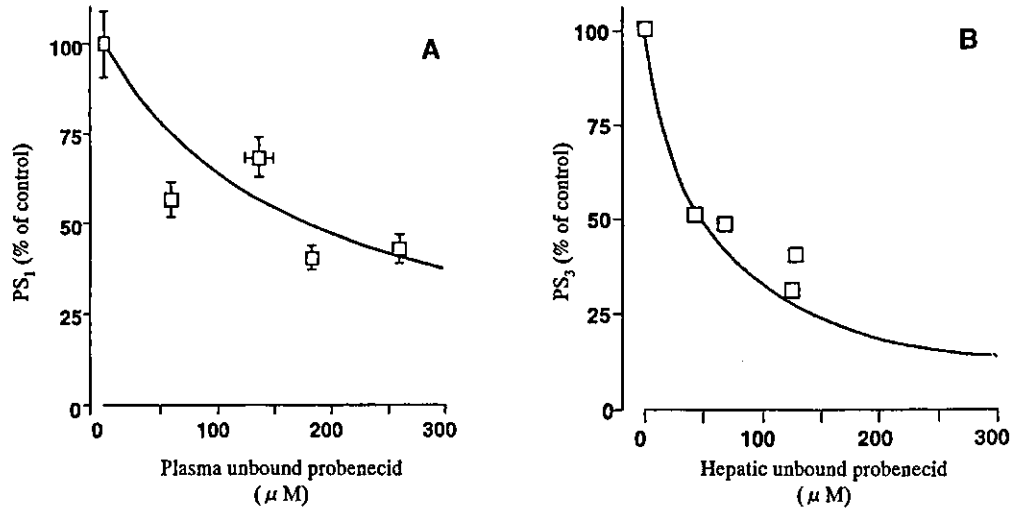

FIG. 6. Extrapolation of the interaction between methotrexate and probenecid across sinusoidal and canalicular membranes in vivo from in vitro data in rats. A, the reduction in the intrinsic clearance for the hepatic uptake of methotrexate across the sinusoidal membrane (PS_1) by probenecid was extrapolated based on eq. 2 of Fig. 5 and is shown as a solid line. The actual PS_1 value (□) obtained from the integration plot analysis was normalized by that in the control, and also plotted. The PS_1 value of the control was 23.9 ± 1.1 ml/min/kg. B, the reduction in the intrinsic clearance for the excretion of methotrexate across the bile canalicular membrane (PS_3) by probenecid was extrapolated based on eq. 3 of Fig. 5 and is shown as a solid line. The actual PS_3 value (□) obtained from the steady-state biliary excretion and hepatic unbound concentration of methotrexate was normalized by that in the control and also plotted. The PS_3 of the control was 60.6 ± 2.4 ml/min/kg (Ueda et al., 2001).

Since it is difficult to measure PS_1 and PS_3 directly in vivo and, in particular, it cannot be estimated in humans in vivo, the degree of inhibition of the net excretion from circulating plasma into bile ($CL_{int,bile}$), expressed by eq. 4 of Fig. 5, has been predicted. It should be noted that there is still only limited information available about the in vitro system that can estimate efflux transport on the sinusoidal membrane (PS_2). In view of this difficulty, a method to avoid false negative predictions, using eq. 5 of Fig. 5, of the interaction involving net biliary excretion has been proposed. If the inhibitor drug also reduces PS_2, the $CL_{int,bile}$ should be increased and, therefore, PS_2 does not need to be considered if we want to avoid any false negative predictions. Thus, in all cases, the reduction in $CL_{int,bile}$ should be, at most, the reduction in PS_1 (sinusoidal uptake) multiplied by that in PS_3 (canalicular efflux) as expressed by eq. 5 of Fig. 5. In actual fact, the predicted values were only slightly lower than the actual values in vivo, suggesting that this method is a suitable way of avoiding any false negative predictions (Ueda et al., 2001). This method can be adapted to the prediction of clinically relevant drug-drug interactions and the calculated R value may be a good criterion for initially investigating the possibility of a drug-drug interaction.

Generally, the substrate specificity of drug transporters is broad and multispecific because they function as detoxification systems. Once the strategy of using drug transporters in the new drug discovery and development processes has been adopted, transporter-mediated drug interactions will always need to be taken into account. However, we believe that pharmaceutical companies should not abandon transporter-based drug discovery, considering it promises greater benefit than risk. We should evaluate which drug candidates are substrates for which transporters, and identify which comedication is likely to cause drug-drug interactions. Furthermore, it is helpful to predict the degree of any changes in pharmacokinetics caused by a drug interaction, using the values of the inhibition constants and clinical concentrations, to provide useful information to clinicians.

IV. Possible Strategies for Drug Discovery Using Drug Transporter Inhibitors

A. P-Glycoprotein Blockade to Overcome Multidrug Resistance

Since over-expression of P-gp or MRP on the surface of tumor cells causes multidrug resistance, the use of a chemomodulator to inhibit efflux transport has been tried in an attempt to overcome this resistance (Cole and Deeley, 1998; Konig et al., 1999a; Kool et al., 1999; Kuwano et al., 1999). Several inhibitors of P-gp, such as PSC-833, LY335979, XR9576, and GF120918, have been discovered and are currently undergoing clinical trials (Ishikawa et al., 2000; Dantzig et al., 2001; Malingre et al., 2001a; Mistry et al., 2001). Since P-gp mediates the biliary and urinary excretion of its substrates (Oude Elferink et al., 1995; Simons et al., 1997) and limits their intestinal absorption (Hunter and Hirst, 1997), inhibition of P-gp will either reduce the hepatic and renal clearance or increase the bioavailability. Thus, some MDR modulators may change not only the concentration of anticancer drugs in tumor cells, but also their plasma concentrations.

Furthermore, it should be noted that P-gp modulators may increase the brain penetration of many drugs, including anticancer drugs, by blocking brain P-gp, leading to CNS side effects (Tsuji and Tamai, 1997; Fromm, 2000; Sadeque et al., 2000; Schinkel, 2001; Troutman et al., 2001). Since the brain is not a clearance organ, it may be that drug interactions involving P-gp will not alter the plasma concentrations, but change only the brain penetration of drugs. In actual fact, the brain distribution of many P-gp substrates is increased significantly in mdr1a knockout mice compared with that in wild-type mice, despite there being only a minor change in the plasma concentrations of these drugs (Table 4). Such cases should be carefully considered because the toxic effect of drugs on the brain cannot be estimated from the change in drug plasma concentrations.

B. P-Glycoprotein Blockade to Improve Efficacy of Human Immunodeficiency Virus Protease Inhibitors

The blockade of P-gp is expected to improve the efficacy of HIV protease-inhibitors (HIV-PIs) (Huisman et al., 2000). Since HIV-PIs are transported by P-gp, their distribution to the target sites is restricted (Lee et al., 1998). P-gp is expressed in several subclasses of lymphocytes, major targets of human immunodeficiency virus type 1 infection (Lucia et al., 1995; Andreana et al., 1996). Cell lines expressing a high level of P-gp significantly reduce the accumulation of HIV-PI, and are less sensitive to HIV-PI antiviral activity than cell lines not expressing P-gp (Turriziani et al., 2000). It is possible that the cells in patients that express P-gp will be relatively resistant to the antiviral effects of HIV-PIs. P-gp is also expressed in the blood-brain and blood-testis barrier and in the materno-fetal barrier formed by placental trophoblasts (Hoetelmans, 1998). Therefore, HIV-PI concentrations in pharmacological sanctuary sites, such as brain, testis, and fetus, are limited by P-gp, and it is assumed that these sites could be a breeding ground for therapy-resistant viruses due to the low drug concentrations (Groothuis and Levy, 1997). Residual viral replication in the CNS is often associated with the acquired immunodeficiency syndrome dementia complex (Achim et al., 1994; Kolson et al., 1998) and that in the testes contributes to the sexual transmission of the infection. Intravenous administration of the novel and potent P-gp inhibitor, LY335979, to mice increased the brain and testes concentrations of nelfinavir up to 37- and 4-fold, respectively (Choo et al., 2000). Oral administration of the P-gp inhibitors valspodar or GG918 completely in-

hibited placental P-gp activity, and the fetal distribution of saquinavir was increased in mice (Smit et al., 1999).

Moreover, P-gp in the small intestine limits the oral bioavailability of HIV-PIs (Kim et al., 1998). Several HIV-PIs, such as saquinavir, have a poor and highly variable oral bioavailability (Perry and Noble, 1998). In addition to rapid metabolism of saquinavir by intestinal and hepatic CYP3A4 (Fitzsimmons and Collins, 1997), intestinal P-gp activity is also likely to be involved in this problem (Kim et al., 1998). It has been reported that coadministration of ritonavir markedly increases the AUC value of orally administrated saquinavir in HIV-infected patients or healthy volunteers (58- and 112-fold, respectively) (Table 11) (Merry et al., 1997; Hsu et al., 1998). Huisman et al. investigated whether the ritonavir effect is primarily mediated by inhibition of CYP3A4 or P-gp (Huisman et al., 2001). In vitro, ritonavir only moderately inhibited P-gp-mediated transport of saquinavir compared with the potent P-gp inhibitor valspodar. When [^{14}C]saquinavir was coadministered orally with the maximum tolerated dose of ritonavir to wild-type and P-gp-deficient mice, saquinavir bioavailability was increased markedly in both strains (Table 11). Furthermore, the brain and fetal penetration of P-gp-deficient mice was markedly higher than that of wild-type mice despite coadministration of a high dose of ritonavir. P-gp still significantly restricts saquinavir penetration into brain and fetus in the presence of ritonavir. These data show that ritonavir is a relatively poor P-gp inhibitor, and the greatly increased bioavailability of saquinavir following ritonavir coadministration most likely results from reduced saquinavir metabolism. Thus, more efficient P-gp inhibitors are needed if one wishes to effectively expose HIV-PIs to pharmacological sanctuary sites.

Effective inhibition of P-gp might improve the oral bioavailability and penetration of HIV-PIs into pharmacological sanctuary sites with the potential to increase the beneficial effects of therapy, but it could also increase unexpected toxicity (Huisman et al., 2003). Careful clinical studies will be needed to establish whether this approach can be applied with a sufficient degree of safety.

V. Species and Gender Differences in Drug Transporters

There is little published information on species differences in drug transporters, although such information is important for predicting human pharmacokinetics. There is a species difference in transport of organic anions via MRP2 across the bile canalicular membrane. The ATP-dependent transport activity (V_{max}/K_m) of the MRP2 substrate DNP-SG in mouse, rat, guinea pig, rabbit, dog, and human CMVs is 25.5, 64.2, 9.4, 8.4, 7.7, and 3.8 μl/min/mg, respectively (Ishizuka et al., 1999). Another report has shown that the transport activity of glutathione conjugates and unconjugated anions (pravastatin, BQ-123, and methotrexate) in human CMVs was ~3- to 76-fold lower than that in rat CMVs, whereas the transport activity of glucuronides was similar in the two species (Niinuma et al., 1999). If there is a marked species difference in transport activity, it will be necessary to predict the in vivo transport activity in humans from in vitro data using human-based experimental systems. The prediction of in vivo transport activity from in vitro data has been successful in animals. For example, Ishizuka et al. have demonstrated that in vivo excretion clearance across the bile canalicular membrane could be predicted by an uptake experiment with CMVs (Ishizuka et al., 1999).

Several transporters have been shown to exhibit gender differences. Although there were only minor gender differences in the expression of rat Oat1 mRNA, rat Oat2 expression in female kidney was considerably higher than in male kidney (Buist et al., 2002; Kobayashi et al., 2002). Conversely, the Oat3 gender difference occurred in liver, rather than kidney, where male mRNA levels were higher than female levels (Buist et al., 2002; Kobayashi et al., 2002). The expression of the gene product for the Ntcp is higher in the liver of male than female rats (Simon et al., 1999). In addition, the uptake of TEA by isolated kidney slices is higher in male than in female rats (Urakami et al., 1999). This is probably caused by the expression levels of rat Oct2 mRNA and the protein in the kidney of males being much higher than those in females (Urakami et al., 1999).

TABLE 11
Saquinavir bioavailability alone and with ritonavir

	Saquinavir Alone	Saquinavir + Ritonavir	Δ	Reference
HIV-infected patients[a]				Merry et al., 1997
C_{max} (ng/ml)	146 (57–702)	4795 (1420–15810)	33× ↑	
AUC_{0-8h} (ng · h/ml)	470 (293–3446)	· 27458 (7357–108001)	58× ↑	
Healthy volunteers[b]				Hsu et al., 1998
C_{max} (ng/ml)	0.07 ± 0.03	2.2 ± 0.5	31× ↑	
AUC_{0-40h} (μg · h/ml)	0.24 ± 0.18	26.8 ± 4.9	112× ↑	
Wild-type mice[c]				Huisman et al., 2001
[^{14}C]saquinavir oral availability (%)	9.1 ± 1.1	232 ± 70	25× ↑	
mdr1a/1b knockout mice[c]				Huisman et al., 2001
[^{14}C]saquinavir oral availability (%)	14.1 ± 2.2	865 ± 105	61× ↑	

[a] 600 mg of saquinavir t.i.d. daily alone and with 300 mg ritonavir b.i.d. Data are median (range).
[b] Single 400 mg of saquinavir alone and with single 600 mg of ritonavir.
[c] 50 mg/kg ritonavir was administered 30 min before oral administration of [^{14}C]saquinavir.

However, there are no gender differences in the mRNA expression levels of rat Oct1 and Oct3 (Urakami et al., 1999).

Oatp1 is localized at the sinusoidal membrane of the liver and the apical membrane of the kidney in the S3 segment of the proximal tubules of the outer medulla (Bergwerk et al., 1996). It has been reported that the expression of Oatp1 mRNA in kidney is approximately 6 times higher in male rats compared with females (Lu et al., 1996). In addition, the urinary excretion of the Oatp1 substrate E_2-17βG is more than 250 times lower in male rats than in females (Table 12) (Gotoh et al., 2002). The urinary clearance with respect to the plasma unbound E_2-17βG in male rats is less than 1% of the glomerular filtration rate, indicating extensive reabsorption from the renal tubules of male rats. A marked increase in E_2-17βG urinary excretion was observed in male rats that had undergone orchidectomy (Table 12) (Gotoh et al., 2002). Testosterone injections given to female rats reduced the urinary excretion to a level comparable with control male rats (Table 12) (Gotoh et al., 2002). A concomitant change in the expression of Oatp1 protein has been found in the kidney membrane fractions following such treatments (Gotoh et al., 2002). These results suggest that urinary E_2-17βG excretion is subject to hormonal regulation and the large gender difference can be explained by the difference in Oatp1-mediated reabsorption. The expression of Oatp1 in the liver does not show any clear gender difference, which is compatible with a minimal gender difference in the uptake clearance of E_2-17βG in the liver (Gotoh et al., 2002). Another report has demonstrated a similar phenomenon in the urinary excretion of taurocholate, dibromosulfophthalein, and zenarestat, an aldose reductase inhibitor, used for the treatment of diabetic neuropathy, in rats (Kato et al., 2002). However, there is still little information about human gender differences in drug transporters.

VI. Synergistic Role of Metabolic Enzymes and Transporters

Both CYP3A4 and P-gp are present at high levels in the villus enterocytes of the small intestine, the primary site of absorption of orally administered drugs (Wacher et al., 2001; Zhang and Benet, 2001). Moreover, these proteins are induced by many of the same compounds and exhibit a broad overlap in their substrate and inhibitor specificities (Wacher et al., 1995), suggesting that they may act synergistically in the small intestine as a barrier to drug absorption (Suzuki and Sugiyama, 2000; Wacher et al., 2001; Zhang and Benet, 2001; Cummins et al., 2002). Recent studies demonstrate that the steroid xenobiotic receptor (SXR), a member of the nuclear hormone receptor superfamily, involved in xenobiotic induction of CYP3A (Bertilsson et al., 1998; Blumberg et al., 1998), can also regulate the expression of the MDR1 gene (Geick et al., 2001; Synold et al., 2001). SXR is activated by paclitaxel and is responsible for inducing the expression of not only CYP3A, but also CYP2C9 and MDR1 (Synold et al., 2001). As paclitaxel is metabolized by both CYP3A4 and CYP2C9 and transported by P-gp, induction of all these proteins leads to its enhanced clearance. This indicates a broad role for SXR in the coordinated induction of multiple detoxification pathways. A similar study of pregnane X receptor (PXR), a mouse ortholog of SXR, has been carried out and shows that PXR regulates the expression of Cyp3a11, Cyp7a1 and Oatp2 (Staudinger et al., 2001a; Staudinger et al., 2001b; Guo et al., 2002). PXR is activated by the toxic bile acid lithocholic acid and its metabolite. Activation of PXR results in the repression of Cyp7a1, which blocks bile acid biosynthesis, and induction of Oatp2 and Cyp3a expression, which promotes bile acid uptake and metabolism. PXR coordinately regulates gene expression to reduce the concentrations of the toxic bile acid lithocholic acid in the liver. Since rifampin and the HIV-PI ritonavir are also ligands for human SXR, they activate the transcription of the CYP3A4 and MDR1 (Dussault et al., 2001; Geick et al., 2001). Coordinated induction of intestinal CYP3A and P-gp via SXR will enhance the ability of a barrier as a detoxification system for xenobiotics in the small intestine. However, the induction of these proteins by drug candidates will potentially cause drug-drug interactions, making successful drug development more difficult. Thus, SXR-binding and -activation

TABLE 12

The gender difference in the urinary excretion of E_2-17βG and the effect of androgen hormone on the urinary excretion of E_2-17βG in rats (Gotoh et al., 2002)

	Male		Female		
	Control	Orchidectomy	Control	Sham[a]	+Testosterone
C_{ss} (fmol/ml)	67.9 ± 3.1	59.2 ± 2.5*	63.4 ± 4.9	64.8 ± 4.7	80.1 ± 3.4†
CL_{tot} (ml/min/kg)	54.2 ± 3.8	63.1 ± 5.1	60.4 ± 4.9	58.1 ± 2.8	45.6 ± 2.3**
CL_{urine} (ml/min/kg)	$<8.2 \times 10^{-3}$	1.27 ± 0.36*	1.11 ± 0.27*	0.919 ± 0.051*	$<9.83 \times 10^{-3}$*†
CL_{bile} (ml/min/kg)	43.9 ± 2.0	49.0 ± 2.8	39.3 ± 6.5	42.1 ± 2.1	45.5 ± 4.1
GFR (ml/min/kg)	11.8 ± 0.8	12.1 ± 0.3	12.0 ± 0.8	9.90 ± 0.30	10.6 ± 0.4

Each value represents the mean ± S.E. of four to five independent experiments during constant intravenous infusion of [^{3}H]E_2-17βG (227 pmol/h/kg) to male and female SD rats.

* Significantly different from control male rats ($P < 0.01$).

** Significantly different from control female rats ($P < 0.05$).

† Significantly different from control female rats ($P < 0.01$).

[a] Vehicle only.

assays are useful tool for screening compounds inducible by CYP3A and P-gp.

Some organic anions (carboxylates), formed by carboxyesterases in enterocytes, are sequentially excreted into the lumen via efflux transporters for organic anions. ME3229 is an ester-type prodrug designed to increase the oral bioavailability of the active carboxylate drug ME3277 (a glycoprotein IIb/IIIa receptor antagonist) (Okudaira et al., 2000b). It has been suggested that the low oral bioavailability of ME3277 (~1% in rats) is related to its low lipophilicity. Although esterification of the carboxylate groups in ME3277 results in a much higher lipophilicity, the oral bioavailability of ME3229 remains comparatively low (~10% in rats). It has been found that ME3229 is rapidly taken up by enterocytes, whereas most of its anionic metabolites (ME3277) produced from prodrugs (ME3229) in enterocytes are actively excreted into the lumen (Okudaira et al., 2000b). High efflux activity located on the luminal membrane, along with the metabolic activity of carboxyesterases in enterocytes, hinders the oral absorption of ester-type prodrugs. This active efflux transport of anionic metabolites is similar in normal rats and Eisai hyperbilirubinemic rats, the latter being hereditarily defective in Mrp2 (Okudaira et al., 2000a). These results show that the anionic metabolites of ME3229 are pumped out into the gut lumen by an energy-dependent transport system distinct from MRP2. It has also been shown that P-glycoprotein is not responsible for this efflux (Okudaira et al., 2000a).

A sequential detoxification system operates on other compounds. Platinum drugs are used widely for chemotherapy of lung cancer, but their effectiveness is limited by resistance. They are metabolized to glutathione conjugates in tumor cells. Intracellular glutathione is formed by γ-glutamylcysteine synthetase and the glutathione conjugates of platinum drugs formed in tumor cells are actively excreted via the ATP-dependent glutathione *S*-conjugate export (GS-X) pump, which has been shown to be identical to MRP. The MRP/GS-X pump and γ-glutamylcysteine synthetase are coordinately induced by exposure to platinum drugs or heavy metals in cisplatin-resistant tumor cells (Ishikawa et al., 1996; Gomi et al., 1997; Oguri et al., 1998). Elevated expression of the MRP/GS-X pump and increased glutathione biosynthesis may both be important factors in the cellular metabolism and disposition of cisplatin.

VII. The Regulation Mechanisms of Drug Transporters

A. The Transcriptional Regulation of Transporters

Knowledge of the regulation of transporters is of great help in predicting pharmacokinetics and drug-drug interactions. As mentioned above, the orphan nuclear receptor PXR (SXR) coordinately regulates drug clearance in response to a wide variety of xenobiotic compounds. Although this signaling system protects the body from exposure to toxic compounds, it can also be a serious barrier to drug therapy. In human hepatocytes, the expression of human MRP2 can be up-regulated by human PXR ligands such as rifampicin (Kast et al., 2002; Kauffmann et al., 2002). In PXR knockout mice, no induction of Mrp2 by pregnenolone 16a-carbonitrile, a ligand for the rodent PXR, has been observed (Kast et al., 2002). This suggests that PXR is involved in the induction of Mrp2 (Kast et al., 2002). In addition, it has been suggested that MRP2 expression is regulated by the farnesoid X-activated receptor (FXR) and constitutive androstane receptor (CAR). Treatment of rodent hepatocytes with the FXR ligand chenodeoxycholic acid or the CAR ligand phenobarbital results in a potent induction of Mrp2 mRNA levels (Kast et al., 2002). The presence of potential PXR, CAR, and FXR binding sites has been demonstrated for human MRP2 (Tanaka et al., 1999; Stockel et al., 2000).

The liver-enriched transcription factor hepatocyte nuclear factor 1 alpha (HNF1 alpha) is critical for hepatocyte-specific OATP-C gene expression. Coexpression of HNF1 alpha stimulated OATP-C promoter activity 30-fold in HepG2 cells and 49-fold in HeLa cells, and mutation of the HNF1 site abolished the promoter function (Jung et al., 2001a). The human OATP8 and mouse Oatp4 promoters were also responsive to HNF1 alpha coexpression in HepG2 cells, suggesting a role for HNF1 alpha as a global regulator of liver-specific organic anion transporter genes (Jung et al., 2001a).

BSEP meditates the ATP-dependent transport of bile salts across the canalicular membrane of hepatocytes and the expression of this transporter is sensitive to the flux of bile acids. Luciferase reporter gene assays have shown that the BSEP promoter is positively controlled by FXR, retinoid X receptor alpha, and bile salts (Plass et al., 2002). FXR/ retinoid X receptor alpha heterodimers specifically bind to the inverted repeat (IR)-1 element in the BSEP promoter (Ananthanarayanan et al., 2001). Reducing endogenous FXR levels using RNA interference fully suppresses bile salt-induced BSEP expression (Plass et al., 2002). FXR is required for the bile salt-dependent transcriptional control of the human BSEP gene.

Recently, an in silico approach has been applied to PXR ligands (Ekins et al., 2002c). Using data for the EC50 values of PXR activation derived for 12 human PXR ligands, a pharmacophore has been developed (Ekins and Erickson, 2002). The pharmacophore was able to distinguish between the most potent activators of PXR and poor activators. The model could be useful in drug development, potentially acting as a high-throughput filter for identifying compounds that may bind to PXR before their in vitro determination. This will aid the selection of molecules with a poor ability to be potent PXR ligands, thereby avoiding the induction of drug-metabolizing enzymes and transporters.

B. The Sorting and Polarization of Transporters

The polarization of cells, such as the epithelial cells lining the bile duct or the kidney proximal tubules, is created largely by the differential localization of specific proteins. To create such polarization, proteins destined for specific membranes have been shown to contain molecular targeting signals. The recent identification of a PDZ-interacting domain in the cystic fibrosis transmembrane conductance regulator (CFTR) is the first report of a targeting motif in mammalian ABC transporters (Moyer et al., 1999). CFTR encoded by the cystic fibrosis gene is localized in the apical membrane of epithelial cells, where it functions as a cyclic AMP-regulated chloride channel and as a regulator of other ion channels and transporters (Kleizen et al., 2000). PDZ-interacting domains in CFTR play a key role in the apical polarization of this transporter in epithelial cells (Moyer et al., 1999). In general, PDZ proteins, which are involved in the apical or basal targeting of membrane proteins, bind to the PDZ-interacting domain characterized by the carboxy-terminal amino acid sequence (Bezprozvanny and Maximov, 2001; Sheng and Sala, 2001). A novel PDZ domain-containing protein, PDZ-K1, binds to the carboxy terminus of human MRP2 (Kocher et al., 1999; Harris et al., 2001). In addition, deletion of carboxy-terminal 15 or more amino acids impairs the localization of MRP2 in polarized HepG2 cells (Nies et al., 2002). The amino acid sequence in this region may be involved in the apical targeting, stabilization, and/or in maintaining the conformation of MRP2 to be released from the ER (Nies et al., 2002).

Under cholestatic conditions, it has been suggested that MRP2 is internalized from the cell surface in rats and humans (Rost et al., 1999; Vos et al., 1999; Paulusma et al., 2000; Shoda et al., 2001; Zollner et al., 2001). Although activation of protein kinase C results in the internalization of MRP2 in HepG2 cells (Kubitz et al., 2001), stimulation by cyclic AMP results in the relocalization of MRP2 in isolated rat hepatocyte couplets (Roelofsen et al., 1998). Under cholestatic conditions, tauroursodeoxycholate stimulates the insertion of internalized MRP2 into the bile canalicular membrane in a protein kinase C-dependent manner (Beuers et al., 2001; Fickert et al., 2001).

Recently, it has been demonstrated that radixin (encoded *Rdx*) was involved in the localization of Mrp2 at bile canalicular membranes (Kikuchi et al., 2002). Radixin is a member of the ezrin-radixin-moesin family of proteins, which cross-link actin filaments and integral membrane proteins. *Rdx* knockout mice ($Rdx^{-/-}$ mice) exhibit marked conjugated hyperbilirubinemia. Interestingly, on the bile canalicular membranes of $Rdx^{-/-}$ mice, the level of Mrp2, which secretes conjugated bilirubin into the bile, is reduced compared with that in wild-type mice, while the expression level of Mrp2 in whole liver did not seem to be reduced in $Rdx^{-/-}$ mice. In addition, in vitro binding studies show that radixin associates directly with the carboxy-terminal cytoplasmic domain of human MRP2. These findings indicate that radixin is required for Mrp2 to localize correctly on the apical membranes in the liver.

The Dubin-Johnson syndrome (DJS) is an inherited disorder characterized by conjugated hyperbilirubinemia. The absence of a functional MRP2 transporter from the apical membrane of hepatocytes explains the molecular basis of this disease (Kartenbeck et al., 1996). Several mutations in the MRP2 gene have been identified in patients with DJS (Paulusma et al., 1997; Tsuji et al., 1999). Keitel et al., have investigated the consequences of a mutation in DJS, which leads to the loss of 2 amino acids from the second ATP-binding domain of MRP2 (Keitel et al., 2000). This mutation is associated with the absence of the MRP2 glycoprotein from the apical membrane of hepatocytes. Transfection of mutated MRP2 complementary DNA leads to an MRP2 protein that is only core glycosylated and located in the endoplasmic reticulum (ER) of transfected cells. This indicates that this mutation leads to impaired maturation and trafficking of the protein from the ER to the Golgi complex. This impaired protein sorting may be responsible for the absence of MRP2 protein from the apical membrane.

VIII. Polymorphisms of Drug Transporters

Selecting drugs and dosages according to genetic and specific individual markers has allowed optimized drug therapy to be developed for individual patients (individualized drug therapy). The possibility of defining patient populations genetically may improve drug safety and efficacy by predicting individual responses to drugs. Nevertheless, it is still desirable to develop drugs that are relatively unaffected by polymorphisms and exhibit little interindividual variability with a wide therapeutic spectrum of activity. Genetic polymorphisms in human membrane transporters may also contribute to interindividual differences in the response to drugs. However, our knowledge of the relevant transporters is limited at present.

Polymorphisms in drug transporters, such as MDR1, MRP1, MRP2, OATP-A, OATP-C, OATP8, OAT1, OAT2, OAT3, OCT2, and OCTN2 have been demonstrated (Nezu et al., 1999; Mayatepek et al., 2000; Cascorbi et al., 2001; Iida et al., 2001; Kerb et al., 2001; Leabman et al., 2002; Suzuki and Sugiyama, 2002; Tirona and Kim, 2002). A number of single nucleotide polymorphisms (SNPs) have been described in the human MDR1 gene (Kim, 2002; Fromm, 2002). An SNP in exon 26 (C3435T) of MDR1 was found to be associated with reduced intestinal expression of P-gp, along with increased oral bioavailability of digoxin (Hoffmeyer et al., 2000). Since C3435T SNP is a silent or "wobble" polymorphism with no amino acid substitutions of the encoded protein, the

mechanism via which this SNP acts on P-gp function remains unclear. Recently, Kim et al. have found that 95% of subjects who were homozygous for the exon 26 C3435T SNP (C/C) were GG homozygous at base position 2677 (Kim et al., 2001). The C3435T SNP in exon 26 appeared to be linked to a G2677T SNP in exon 21. The G2677T transversion in exon 21 resulted in an alteration in the encoded protein (Ala893Ser). In vitro expression of MDR1 encoding Ala893 (MDR1*1) or a site-directed Ser893 mutation (MDR1*2) led to enhanced efflux of digoxin by cells expressing the Ser893 variants (Kim et al., 2001). Moreover, subjects with the C3435T and G2677T allele (MDR1*2) have over a 40% lower AUC value following oral administration of fexofenadine, a P-gp substrate, compared with subjects with the MDR1*1 variant (Table 13) (Kim et al., 2001). This is consistent with the in vitro data and suggests enhanced in vivo P-gp activity among subjects with the MDR1*2 allele. This finding contradicts previous results about the effect of exon 26 C3435T SNP on digoxin disposition (Hoffmeyer et al., 2000). The reason for this discrepancy and failure to detect exon 21 SNP in a previous study is currently unclear. A polymorphism of MDR1 may change the expression level and/or functional activity of P-gp in the brain as well as that in the small intestine, and contribute to interindividual differences in the brain penetration of P-gp substrates. It is possible that the change in the brain penetration of P-gp substrates caused by P-gp SNPs is more marked than that in the small intestine and may affect interindividual differences in the degree of CNS toxicity exhibited by P-gp substrates. However, assessment of the role of P-gp in BBB function in humans is problematic, since brain concentrations cannot be measured readily. A key area for future investigation of the role of human P-gp in the BBB will be the development of a suitable probe substrate appropriately labeled for continuous monitoring of brain penetration using positron emission tomographic imaging techniques (Hendrikse et al., 2001).

OATP-C is a liver-specific transporter involved in the hepatocellular uptake of a variety of clinically important drugs. The presence of multiple functionally relevant SNPs in OATP-C has been reported (Tirona et al., 2001; Michalski et al., 2002; Nozawa et al., 2002; Tirona and Kim, 2002). In vitro experiments with cultured cells expressing the wild-type and mutated OATP-Cs revealed that several variants exhibited markedly reduced uptake of the OATP-C substrates estrone sulfate and E_2-17βG (Tirona et al., 2001) (Table 14). Specifically, alterations in transport were associated with the SNPs that introduce amino acid changes within the transmembrane-spanning domains and with those that modify extracellular loop 5, suggesting an important role of this region in any substrate-transporter interaction (Table 14). Furthermore, several OATP-C variants were found to have reduced fractional cell membrane expression compared with the wild-type allele (Tirona et al., 2001; Michalski et al., 2002; Nozawa et al., 2002). Interestingly, the variant with A1964G SNP reduced the transport activity of estrone sulfate but not that of E_2-17βG, suggesting possible substrate-dependent polymorphisms. A similar phenomenon has been found in SNPs of polyspecific organic cation transporter OCT1 (Kerb et al., 2002). The Cys88Arg and Gly 401Ser mutants could mediate significant uptake of TEA and serotonin, although they were unable to transport 1-methyl-4-phenylpyridinium (MPP). These mutants exhibit an altered substrate selectivity. In such a case it is possible that the transport activities of some drug candidates can be altered by some SNPs, even if those of typical substrates are unaffected by the SNPs. If so, it will be necessary to evaluate every drug candidate in terms of the transport activity of each variant. Recently, Nishizato et al. have investigated the contribution of the genetic polymorphisms of the OATP-C gene to the pharmacokinetics of pravastatin, a substrate for OATP-C (Nishizato et al., 2003). Among 120 healthy Japanese individuals, five nonsynonymous variants were observed in the OATP-C gene. Subjects with the OATP-C*15 allele (Asp130Ala174) had a reduced total and nonrenal clearance compared with those with the OATP-C*1b allele (Asp130Val174); nonrenal clearance in *1b/*1b (n = 4), *1b/*15 (n = 9), and *15/*15 (n = 1) subjects was 2.01 ± 0.42, 1.11 ± 0.34, and 0.29 (l/h/kg). Mean serum concentration-time curves of pravastatin were different among the three genotypic groups with regard to the *15 allele (Fig. 7). T521C (Val174Ala) SNPs are likely to be associated with altered pharmacokinetics of

TABLE 13
MDR1 alleles and fexofenadine disposition (Kim et al., 2001)

Genotype	Subjects		$AUC_{(0-4)}$ (ng · ml^{-1} · h)	C_{max} (ng · ml^{-1})	T_{max} (h)	$T_{1/2}$ (h)
	No.	%				
Caucasian (n = 37)						
*1/*1	6	16	1316 ± 543	508 ± 205	2.7 ± 0.8	2.8 ± 0.4
*1/*2	4	11	1171 ± 967	400 ± 282	3.3 ± 1.0	3.1 ± 0.7
*2/*2	5	14	837 ± 311	317 ± 185	2.4 ± 1.7	3.5 ± 0.9
African-American (n = 23)						
*1/*1	9	39	1030 ± 435	386 ± 163	1.9 ± 0.9	3.3 ± 0.3
*1/*2	3	13	1099 ± 70	405 ± 29	2.3 ± 1.2	2.7 ± 0.4

180 mg fexofenadine was administered orally. The MDR1*2 allele contain 3 SNPs simultaneously; C1236T in exon 12, G2677T in exon 21, and C3435T in exon 26. The first published MDR1 sequence is shown as the MDR1*1 allele.